DOKUZ EYLÜL UNIVERSITY
GRADUATE SCHOOL OF NATURAL AND APPLIED SCIENCES

CHIRP SPREAD-SPECTRUM BASED DIGITAL COMMUNICATION UNDER NON-GAUSSIAN NOISE CHANNELS

by
Zafer KARAÇOKAK

December, 2016
İZMİR

CHIRP SPREAD-SPECTRUM BASED DIGITAL COMMUNICATION UNDER NON-GAUSSIAN NOISE CHANNELS

A Thesis Submitted to the
Graduate School of Natural and Applied Sciences of Dokuz Eylül University
In Partial Fulfillment of the Requirements for the Degree of Master of Sciences
in Electrical and Electronics Engineering Program

by
Zafer KARAÇOKAK

December, 2016
İZMİR

GAUSS OLMAYAN GÜRÜLTÜLÜ KANALLARDA CHIRP YAYGIN BANDLI SAYISAL HABERLEŞME

Dokuz Eylül Üniversitesi Fen Bilimleri Enstitüsü
Yüksek Lisans Tezi
Elektrik Elektronik Mühendisliği Anabilim Dalı

Zafer KARAÇOKAK

Aralık, 2016
İZMİR

M.Sc THESIS EXAMINATION RESULT FORM

We have read the thesis entitled **"CHIRP SPREAD-SPECTRUM BASED DIGITAL COMMUNICATION UNDER NON-GAUSSIAN NOISE CHANNELS"** completed by **ZAFER KARAÇOKAK** under supervision of **ASST. PROF. DR. M. EMRE ÇEK** and we certify that in our opinion it is fully adequate, in scope and in quality, as a thesis for the degree of Master of Science.

Asst. Prof. Dr. M. Emre ÇEK

Supervisor

Assoc. Prof. Dr. Olcay AKAY

(Jury Member)

Asst. Prof. Dr. İlhan BAŞTÜRK

(Jury Member)

Prof. Dr. Ayşe OKUR
Director
Graduate School of Natural and Applied Sciences

ACKNOWLEDGMENTS

Firstly, I would like to extend my sincerest gratitude to my supervisor, Asst. Prof. Dr.M. Emre ÇEK, for his help, precious advices, guidance and encouragement throughout the entire duration of my thesis studies at Dokuz Eylul University. Without his time, encouragement, efforts, and knowledge, this thesis would not have been completed. I could not wish for friendlier supervisors.

Secondly, of course, the greatest appreciation of all goes to my family whose insightful advice, strongest support, understanding and patience inspired me to overcome any hurdles in my way.

Zafer KARAÇOKAK

CHIRP SPREAD-SPECTRUM BASED DIGITAL COMMUNICATION UNDER NON-GAUSSIAN NOISE CHANNELS

ABSTRACT

The purpose of this thesis is to determine the properties of chirp spread-spectrum to link secure communications under non-gaussian noise channels. The thesis includes not only analysis of performances of chirp modulated spread-spectrum communication system performance but also the error performance in presense of both Gaussian and symmetric α-stable ($S\alpha S$) distributed noise.

The conventional direct sequence spread-spectrum communication systems and chirp modulation based communication system construct basis for analysis of chirp spread-spectrum under stable distributions.

Two chirp signaling, known as chirp-binary orthogonal keying (Chirp-BOK) and antipodal chirp keying techniques are analyzed under different noise distributions in the thesis study.

Thesis study has the contribution on effect of impulsive channels on chirp spread-spectrum (CSS) systems. It is concluded that the increasing impulsive behaviour of the channel causes error performance to decrease.

Keywords: Gaussian noise, chirp-binary orthogonal keying, antipodal chirp keying, alpha-stable (α-stable) noise, generalized signal-to-noise ratio (GSNR).

GAUSS OLMAYAN GÜRÜLTÜLÜ KANALLARDA CHIRP YAYGIN BANDLI SAYISAL HABERLEŞME

ÖZ

Bu tezin amacı Gauss olmayan gürültülü kanallar altında güvenli sayısal haberleşmeler kurmak için chirp yaygın bant spektrumun özelliklerini belirlemektir. Tez sadece chirp modülasyonlu yaygın bant spektrum haberleşme sistem performans analizini değil aynı zamanda Gauss ve simetrik α-kararlı dağılmış her iki gürültü durumundaki hata performansını da kapsamaktadır.

Konvansiyonel doğrudan sıralı yaygın bant spektrum haberleşme sistemleri ve chirp modülasyon tabanlı haberleşme sistemi kararlı dağılımlarda chirp yaygın bant spektrumun analizine temel oluşturmaktadır.

Chirp ikili ortogonal anahtarlama (Chirp-BOK) ve zıt yönlü chirp anahtarlama teknikleri olarak bilinen iki chirp sinyal türü farklı gürültü dağılımları altında tez çalışmasında analiz edilmektedir.

Tez çalışmasının chirp yaygın bant spektrum (CSS) sistemlerinde dürtüsel kanalların etkisi ile ilgili katkıda bulunmaktadır. Kanalın artan dürtüsel davranışının hata performansının azalmasına sebep olduğu sonucuna varılmaktadır.

Anahtar kelimeler: Gauss gürültü, chirp-ikili ortogonal anahtarlama, zıt yönlü chirp anahtarlama, alfa-kararlı (α-kararlı) gürültü, genelleştirilmiş işaret-gürültü oranı (Ing. GSNR).

LIST OF FIGURES

TABLE OF CONTENTS

CHAPTER ONE
INTRODUCTION

Spread-spectrum communication systems are suitable for performing a robust communication link between transmitter and receiver in highly disturbed noisy radio environments. In spite of originating for military purposes, spread-spectrum is a popular technology covering various areas of digital and mobile communications. Conventionally, these techniques consist of direct sequence spread-spectrum (DSSS), frequency hopped spread-spectrum (FHSS), time hopped spread-spectrum (THSS) systems and chirp spread-spectrum (CSS).

Chirp pulses are actually used in nature by dolphins and bats. In 1940, these pulses were first patented for radar applications by Prof. Huttmann, and were further developed by Sidney Darlington (Lifetime IEEE Fellow) in 1947 as Pulse Compression Radar (Nanotron.com). Usage of chirp waveform based wireless communication system for binary signaling goes back to 1962. In a historical point of view, chirp modulation basically employed one pair of linear frequency modulation having different chirp rates in order to encode the binary information. It was reported by (Hengstler et al., 2002) that Gott and Newsome, in 1971, designed a communication system with chirp modulation which operated in the high frequency band and measured carrier interference together with system's bit error rate (BER) in Additive White Gaussian Noise (AWGN). In 1974, the study of Winkler was further developed by Cook to allow several users for multiple access. (El-Khamy et al.,1996) expanded Cook's this study for chirp signals which selected users with the same power and bandwidth in 1996.

CSS, used in radars and sonars, is based on the pulse compression technique with its high processing gain and strong domination. CSS has still kept on to perform different modulation schemes to maintain its immunity against interference from noise and jamming, in wireless communications. Nowadays, various modulation types are widely used in CSS systems for military communications. The most common ones are Binary Orthogonal Keying (BOK) (Wang, 2008) and Chirp Binary Phase Shifted Keying (Chirp-BPSK), operated on indoor and industrial wireless applications. There have been many articles concerning with CSS briefly described in the sequel.

The problem of the parameter estimation of chirp signals was addressed in 1990s. (Djuric & Kay,1990) estimated chirp rate, frequency and phase of the signal in noise and stated that the proposed estimator was unbiased and reaches Cramer-Rao lower bound for reasonable signal to noise ratios (SNR). Later, design and performance of a low-cost wireless broadband chirp communication system using surface acoustic wave delay lines (SAW DLL) based on expansion and compression filters were examined for indoor and industrial environments. Chirp signals were analyzed via a hardware demonstrator with SAW based chirp BOK in which data transfer due to the limiting factors achieved up to 5 Mb/s in (Springer et al.,1998). Shortly afterwards, BOK based Pulse Position Modulation (PPM), BOK and $\pi/4$-Differential Quadrature Phase Shift Keying ($\pi/4$-DQPSK) schemes were explored by (Springer et al., 2000) in order to overcome distortion by frequency selective fading and continuous wave (CW) interferers in indoor environments. The performances of these modulation techniques were illustrated by BER graphs under AWGN channel. Following the study of (Springer et al., 1998), (Springer et al., 2001) combined chirp signals and $\pi/4$-DQPSK modulation to increase data transmission rate and improve the carrier recovery of QPSK systems.

Simic et al. (2001) studied reducing intersymbol interference by designing compression filters to decrease the side lobe effects and correspondingly, increase the error performance which is based on iterative reweighted least square (IRLS) algorithm to keep the width of main lobe fixed. On the other hand, the study of (Djuric & Kay, 1990) was further developed to overcome the problem of parameter estimation of superimposed chirp signals in noise by (Saha & Kay, 2001) which employs the non-iterative maximum likelihood (ML) technique to estimate the complex amplitudes, chirping rates, and frequencies. (Hengstler et al., 2002) proposed a different method in Chirp Modulation Spread Spectrum (CMSS) for multiple access. This method generated antipodal signals with the proper parameters of the linear chirps to reduce the multiple access interference (MAI) under AWGN channels. In conventional DSSS, chirp signals may act as interfering components to reduce the performance of conventional spectrum spreading. The study of (Sahmoudi & Meraim, 2004) tried to model multi-component chirp signals as interfering signals and had an attempt on analyzing the effect of impulsive noise having $\alpha -$stable distribution as channel model. The proposed algorithm utilized a proper time-frequency distribution (TFD) in which the signal components were separated and their corresponding IFs were estimated. As a comparison of the study of (Saha & Kay, 2001) which employs importance sampling to estimate superimposed chirp signals in noise, (Lin et al., 2004) proposed an approach utilizing Markov Chain Monte Carlo (MCMC) algorithm to estimate the parameters of multiple chirp signals. Cramer-Rao lower bound was also achieved at low SNR compared with (Djuric & Kay, 1990). In order to increase data transmission rate, (Huang et al., 2005) proposed *M*-ary chirp spread spectrum (MCSS) modulation achieved by assigning different chirp rates with different sign and magnitude, and a bank of correlators were employed for underwater acoustic (UWA) communication. When combining Differential Phase Shift Keying (DPSK) modulation and the time overlapping, MCSS achieved higher data rate and larger processing gain in low BER range. Considering wireless channel model, (Zhang & Liu, 2006) analyzed an ultra-wide-band (UWB) communication system using high order modulation CSS transmission technique such as a Direct Modulation (DM) using $\pi/4$-DQPSK and Quadrature Amplitude Modulation (QAM). This system was immune to Doppler frequency offset under multi-path environment and was robust against ISI and high envelope variation caused by overlap without loss of the bit rate in existing CSS systems. One of the main studies on CSS in wireless communication has been constituted by (Wang et al., 2008) who investigated CSS by performing Chirp-BOK and multi-user Chirp-BOK modulations in AWGN channel model. Subsequently, (Yu et al., 2009) proposed a special time-varying cross fourth order moment method to estimate the time delay of multi path chirp signals. Differing from previous studies (Lee et al., 2009) analyzed the symbol error rate (SER) performance of a CSS based DM-*M*-ary Phase Shift Keying (MPSK) system in the presence of broadband and tone jamming signals. In (Lakshminarayana et al., 2009), an efficient Fractional Fourier Transform (FrFT) technique was proposed to reduce MAI for Linear Frequency Modulated

(LFM) applications. A CMSS receiver based on FrFT was utilized in AWGN for multiple access system design in which multiple chirp signals were assigned. Augmenting the methods utilized in previous studies, (Zhang & Tao, 2010) described a hybrid spread-spectrum technique involving CSS and FHSS where Short-time-Fractional Fourier Transform (STFrFT) was used to detect and estimate parameters at the receiver. In another application of FrFT in CSS, (Zhao et al., 2010) proposed a Multiple Chirp-rate Shift Keying (MCrSK) modulation scheme based on FrFT utilizing different chirp-rates. This modulation showed better performance than MQAM and MPSK using different chirp-rates for symbols. Nonlinear frequency modulation obtained by chaotic signals has been also the subject of CSS communication systems in order to provide covertness. For this purpose, BER performance of Chaotic CSS (CCSS) system under multi-path channels were analyzed by (Salih, 2010) in which the proposed system with QPSK modulation scheme and a matched filter using adaptive threshold decision were employed to reduce the multi-path fading effects. As the extension of (Huang et al., 2005), (He et al., 2010) stated that MCSS-DPSK method combining DPSK and time overlapping was used to increase the data rate and MCSS-DPSK performance with Rake receiver was robust in multi-path underwater acoustic channel, comparing Chirp-DPSK/DQPSK with and without Rake receiver. Having the same motivation, (Yifeng et al., 2010) described an efficient and fast algorithm used to estimate multi-path delay for additive colored noise in CSS system. This estimation algorithm was reported to have high precision and utilized the fourth-order cumulant matrix decomposition by a Multistage Wiener Filter (MSWF) to calculate the number of multi-path according to the specification defined in IEEE 802.15.4a. Following this study, (Dotli´c & Kohno, 2011) investigated the Impulse Radio Ultra-Wideband (IR-UWB) system modeled by linear chirp UWB pulses as symbols in multi-path channels. When BER performance between chirp and sampling receivers were compared with each other considering different durations of the transmitted signals to analyze the robustness of the system multi-path performance in the channel, it has been declared that the Time-Bandwidth (TB) product looked almost independent of the duration of the transmitted signal. Unlike the study of (Sahmoudi & Meraim, 2004), (Guo et al., 2011) proposed an algorithm with proper noise rejection ability and applicable to estimate the parameters of multicomponent chirp signals in highly disturbed noise environment. In this study, the signal was decomposed into time frequency components using Gabor function, named as Gabor atoms, and the multicomponent signal parameters were estimated by using Hough transform so that there has been no need to compute time-frequency distribution in strong interference and colored noise. Chirp signal can be modified in order to provide adaptability for multiple access based Wireless Personal Area Network (WPAN) system introduced by (Fanyu & Xuemai, 2011) yields satisfactory BER performance for multiple access in AWGN channel and the channel specified by IEEE 802.15.4a standards.

One of the critical aspect on chirp spread spectrum is to extend the chirp modulated digital communication of M-ary communication system in order to increase the data transmission rate. A critical study performed by (Kadri et al., 2011) presented detection and performance of weak M-ary CSS (MCSS) signals in Middleton's Class-A noise. The optimal weak signal receiver with a Zero-Memory Nonlinearity (ZMNL) function performed well to detect MCSS signals in Class-A impulsive non-Gaussian noise model, the Locally Optimal Bayes Detector (LOBD) for MCSS signals was used in the impulsive noise model and BER performance of MCSS modulations are compared. Subsequently, two non-linear UWB chirp waveforms were proposed by (Bai et al., 2012) to reduce the narrow band interference (NBI) in UWB systems. The Direct Sequence Pulse Binary Amplitude Modulation (DS-BPAM) UWB systems based on the proposed chirp waveforms achieved excellent NBI suppression performance, compared to UWB system based on the linear chirp waveform. In the motivation of wireless communication, (Billa et al., 2012) performed an efficient CSS multiple access technique. This technique with inherent interference rejection capability was immune to Doppler shift and multi-path fading especially in certain circumstances. Related with the study by (Kadri et al., 2011), non-coherent detection of the chirp signals in non-Gaussian impulsive noise was applied by (Kadri., 2012). On the other hand, (Cong-ren et al., 2013) pointed out an improved modulation scheme such as BOK-Quaternary Binary Orthogonal Keying (QBOK) giving double bit rate under UWA conditions, instead of a chirp waveform only representing one bit information as in BOK scheme.

Similar to this study, (Khan et al., 2013) presented the BER performance of a class of chirp signals for M-ary data transmission as M-ary chirp modulation (MCM) over Nakagami-m frequency selective channels and non-selective fading channels such as Rayleigh and Nakagami-m flat fading.

As given in (Kadri et al., 2011; 2012) partially, various optimum receivers are modeled to increase the detection performance under $S\alpha S$ distributed interference mixed by AWGN since noise cannot be considered as AWGN.

Differing from the given channel characteristics, the linear combination of both Gaussian and symmetric α-stable noise ($S\alpha S$) are considered to be resulting channel noise and several detector types and a novel sub-optimum detector is proposed by (Sureka & Kiasaleh, 2013). As the following study, the BER performances of differential PSK (DPSK), differentially encoded PSK (DEBPSK) and offset QPSK (OQPSK) in $S\alpha S$ noise are described in analytical form by (Yang & Zhang, 2014). It is reported that the impulsiveness of the channel has certain effect which reduces the error performance. Since the skewness of the stable distribution is always assumed to be symmetric, there is no satisfactory study about the effect of the skewness of the noise on communication performance.

CHAPTER TWO
CHIRP SPREAD SPECTRUM

To protect the secrecy and security of the information-bearing signal in noisy environment or disturbed channels is vital. In the recent years, several different techniques have been applied on the baseband signal to camouflage the message against intruders. Spread spectrum communication has been one of the major mentioned techniques which not only provides certain level of covertness but also satisfactory robustness against interference could be achieved in multi-user communication systems. Before discussing chirp spread spectrum (CSS), it is more convenient to define conventional spread spectrum concept and give information in detail about only direct sequence spread spectrum (DSSS) among several spectrum-spreading techniques such as frequency-hopped spread spectrum (FHSS), chirp spread spectrum (CSS), and a hybrid-structure spread spectrum.

2.1 Background

Basically, spectrum-spreading is a way of hiding the baseband signal. Bandwidth is distributed by diffusion into a wider bandwidth via a noise-like behaving signal which is named as pseudo noise (PN). This spectrum-spreading operation causes the transmitted signal’s spectrum to appear as broadband. A measure to represent the spectrum-spreading performance is processing gain which is expressed as the ratio of symbol duration and the PN chip duration in logarithmic scale. Processing gain (in dB) can be commonly in ranges between 10 dB and 60 dB in a typical spread spectrum system (Maximintegrated.com). Spread-spectrum is related to the extension of transmitted signal bandwidth. As an illustration, typical spread-spectrum communication system is shown in Figure 2.1. Differing from the conventional communication system, the PN sequence which is identical and synchronized between transmitter and receiver provides the communication system to be enabled for multiuser communication and covertness.

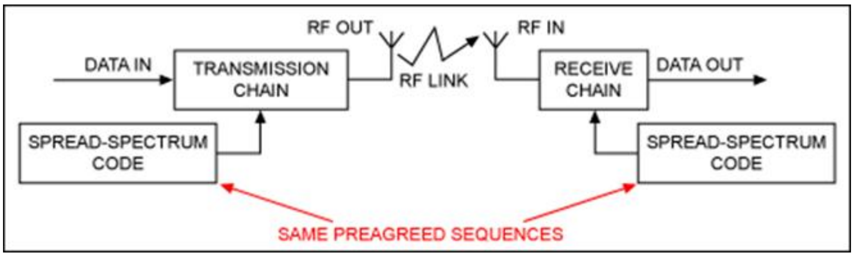

Figure 2.1 Spread-spectrum communication system (Tutorial 1890, An Introduction to Spread-Spectrum Communications, n.d.)

The vital part is that a special binary PN sequence code is generated at the transmitter side, and it is known by the receiver in order to recover the raw binary message. The main property of this PN sequence is the orthogonality within a certain bit duration.

As mentioned in the beginning of this section, DSSS system involves a pseudo noise sequence which is binary in terms of non-return to zero (NRZ) signaling form. It has a common circuitry composed by linear feedback shift register including D-type flip-flops and logic circuit consisting of modulo-2 adders to alternate the states of the m-length flip-flops with respect to the clock pulses as illustrated in Figure 2.2. The period of a PN sequence is determined by the spreading factor. It is a function of flip flops and can be maximum, $N = 2^m - 1$. When the code length is $2^m - 1$, the PN code is called maximal length sequence.

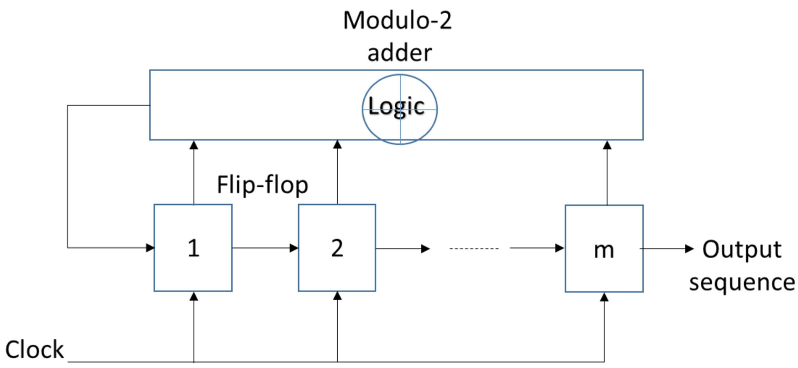

Figure 2.2 Feedback shift register with m-length flip-flops (Haykin, 2001)

A basic DSSS system can be illustrated in time domain using message signal $b(t)$ including two bits $\{+1, -1\}$ of binary information with bit duration T_b, bit energy E_b, PN spreading code $c(t)$ and spreaded message $m(t)$ shown in Figure 2.3(a), (b) and (c), respectively. The carrier signal conventionally shifts the spread signal into the bandpass domain. Figure 2.3(d) represents the time domain high frequency sinusoidal carrier and the Figure 2.3(e) illustrates the direct sequence - binary phase shift keying (DS/BPSK) signal according to BPSK modulation type. This illustration can be extended to different modulation techniques. The spectrum-spreading is performed by the spreading code $c(t)$. The basic property of this code is to exhibit a non-predictable behavior in time domain. Correspondingly, one could expect to observe an autocorrelation function resembling the autocorrelation of noise.

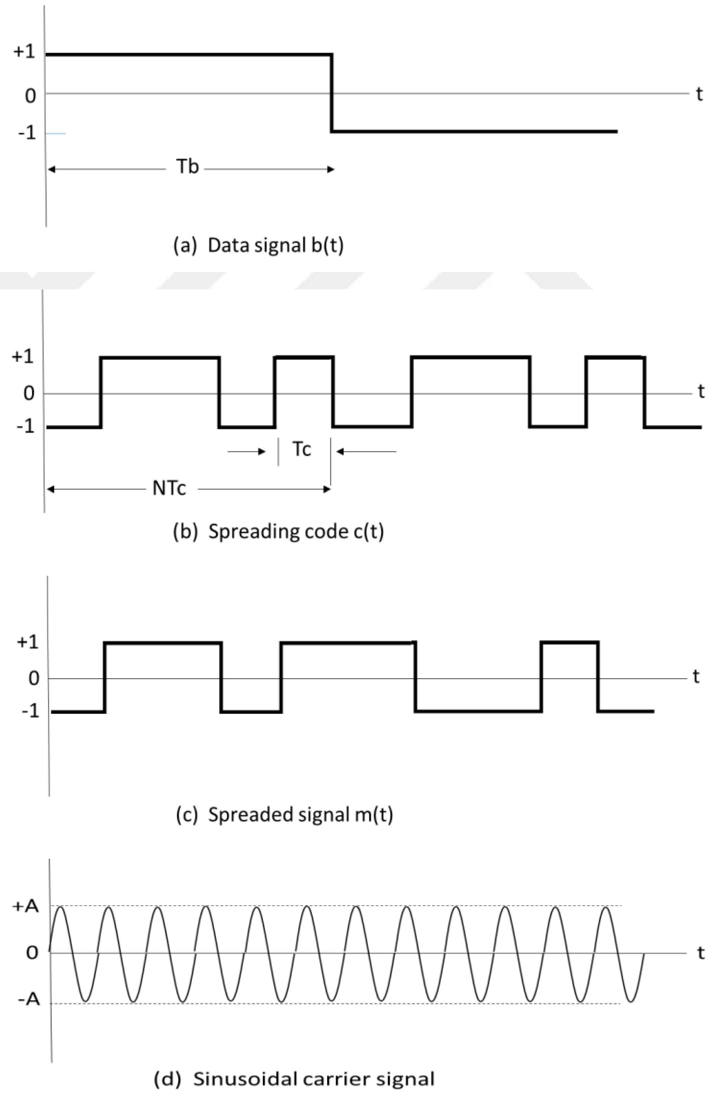

Figure 2.3 (a) Data signal, (b) Spreading PRN code, (c) Spreaded signal (d) Sinusoidal carrier signal and (e) DS/BPSK signal in the transmitter stage (Haykin, 2001)

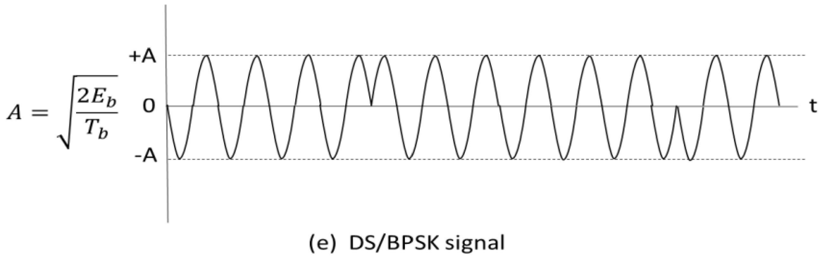

Figure 2.3 (a) Data signal, (b) Spreading PRN code, (c) Spreaded signal (d) Sinusoidal carrier signal and (e) DS/BPSK signal in the transmitter stage (Haykin, 2001) (Continue)

On the other hand, the noise-like autocorrelation behavior of spreading code signal should be achieved in every chip duration T_c. The autocorrelation function of the code signal $R_c(\tau)$ is given as follows

$$R_c(\tau) = \frac{1}{T_b}\int_{-T_b/2}^{T_b/2} c(t)c(t-\tau)dt \tag{2.1}$$

where $-\frac{T_b}{2} \leq t \leq \frac{T_b}{2}$ and the correlation function is periodic with period NT_c. The processing gain (PG) is expressed for DSSS systems mathematically as $G(dB) = 10\log\left(\frac{T_b}{T_c}\right) = 10\log\left(\frac{NT_c}{T_c}\right) = 10\log N$, proportional with length of sequence N, if the spread-spectrum communication system architecture is chosen to yield maximal length sequence. Figure 2.4 illustrates the autocorrelation function of $c(t)$. One can clearly observe that, although it is informed that noise-like behavior is exhibited by a PN sequence, it is valid only within the symbol duration.

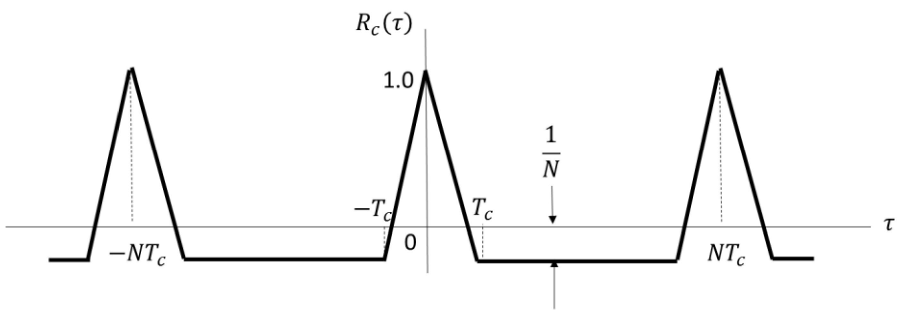

Figure 2.4 Autocorrelation function of spreading sequence $c(t)$ (Haykin, 2001)

The transmitted baseband signal is mathematically found by multiplying the narrow-band message signal with the spreading code signal as given below

$$m(t) = b(t) * c(t). \quad (2.2)$$

By adding additive white Gaussian noise (AWGN) signal $n(t)$, or in other words the interference in the channel, yields the received signal $r(t)$ to be observed in baseband domain as

$$r(t) = m(t) + n(t). \quad (2.3)$$

In the receiver, the received signal $r(t)$ is multiplied again with the same code signal known by the receiver and the resultant signal $z(t)$ is obtained as in Eq. (2.4)

$$z(t) = c(t) * r(t). \quad (2.4)$$

Since $c(t)[b(t) \cdot c(t) + n(t)]$ contains $c^2(t) = 1$, for all t, the demodulator output can be reduced to Eq. (2.5)

$$z(t) = b(t) + c(t) * n(t). \quad (2.5)$$

By integrating over a bit interval for $-\frac{T_b}{2} \leq t \leq \frac{T_b}{2}$, $z(t)$ is low-pass filtered and the term $c(t) * n(t)$ is neglected to correlate the information-bearing data bits properly. Decision factor, v is calculated and compared with the threshold whose level is zero due to NRZ bipolar signaling. Thus, a decision is produced to determine whether the bit symbol is '1' or '0' with respect to the threshold level. Block diagram of conventional DSSS system with BPSK modulation scheme is shown in Figure 2.5, (Haykin, 2001).

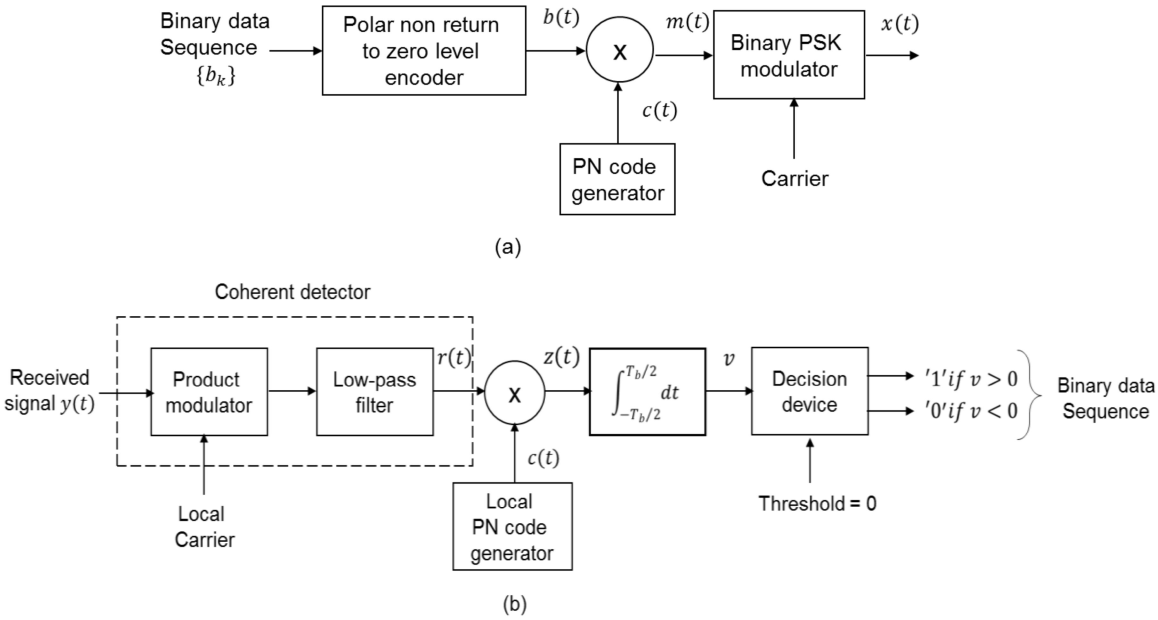

Figure 2.5 (a) The transmitter stage and (b) the receiver stage in DSSS system with coherent BPSK scheme (Haykin, 2001)

Similarly, other different techniques can also be applied according to the point at which a PN sequence tunes the frequency of the communication system as illustrated in Figure 2.6. Differing from DSSS which modulates the baseband data via PN sequence, the second type of spread spectrum communication known as the frequency-hopping spread spectrum (FHSS) utilizes the PN codes in order to hop the carrier-frequency, when applied at the local oscillator (LO) stage.

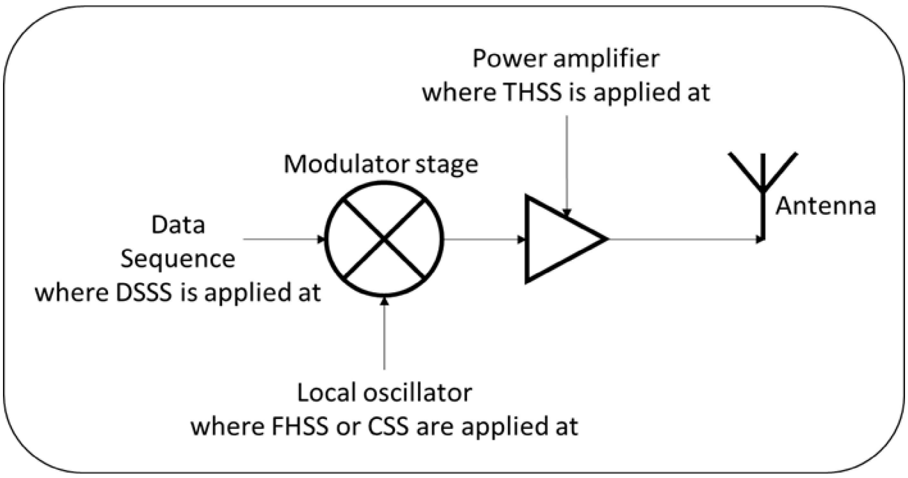

Figure 2.6 Several other spreading techniques applied at different stages in the transmitter

Finally, there is also the "chirp" technique which linearly sweeps the carrier frequency in time. Chirp spread spectrum (CSS) can be considered as spread-spectrum technique which maps the narrow-band message into linear or non-linear frequency modulated signal, known as chirp signals and are used to transmit the binary information. Although they are most commonly used in radar signal processing in order to identify the parameters of target such as altitude, location, and speed, they are widely used in spread spectrum communications as information bearing signal with low power consumption, robustness against interference and multi-path effects or jamming signal due to acting as a superposition of multiple sinusoidal signals with different frequencies (Maximintegrated.com).

In a typical CSS communication system, there are several ways to transmit the binary information in chirp waveform. In the sequel, brief information is given about basic linear chirp signal and a few different chirp modulation techniques.

2.2 Chirp Theory

Theoretically, a conventional linear chirp waveform is linear frequency modulated signal described as follows

$$s(t) = A\,cos[\theta(t)] = A\cos[2\pi f_c t + \pi\mu t^2 + \varphi_0] \qquad (2.6)$$

where A, θ, f_c, μ, and φ_0 are the amplitude, angle, carrier frequency, chirp rate, and phase components, respectively (Springer et al., 2000). The instantaneous frequency of the chirp waveform is given as

$$f_{inst} = \frac{1}{2\pi}\frac{d\theta(t)}{dt}. \qquad (2.7)$$

Assuming that the initial phase is zero, the instantenous frequency of conventional chirp waveform in Eq. (2.6) can be found as

$$f_{inst} = \frac{1}{2\pi}\frac{d(2\pi f_c t + \pi\mu t^2)}{dt} = f_c + \mu t. \tag{2.8}$$

Since the instantenous frequency is a linear function of time, it is called as linear chirp waveform. The rate of variation of instantaneous frequency is described as chirp rate which is given in Eq. (2.9) below

$$\mu = \frac{df_{inst}(t)}{dt} = \frac{d^2\theta(t)}{dt^2} \tag{2.9}$$

As an illustration, chirp waveforms having increasing and decreasing chirp rate together with instanteous frequencies are shown in Figure 2.7 where duration of chirp signal T_c represents bit duration ($T_c = 1\ \mu sec$), carrier frequency f_c is taken to be $f_c = 20\ MHz$ and the bandwidth is given to be $B = |\mu|T_c = 4\ MHz$.

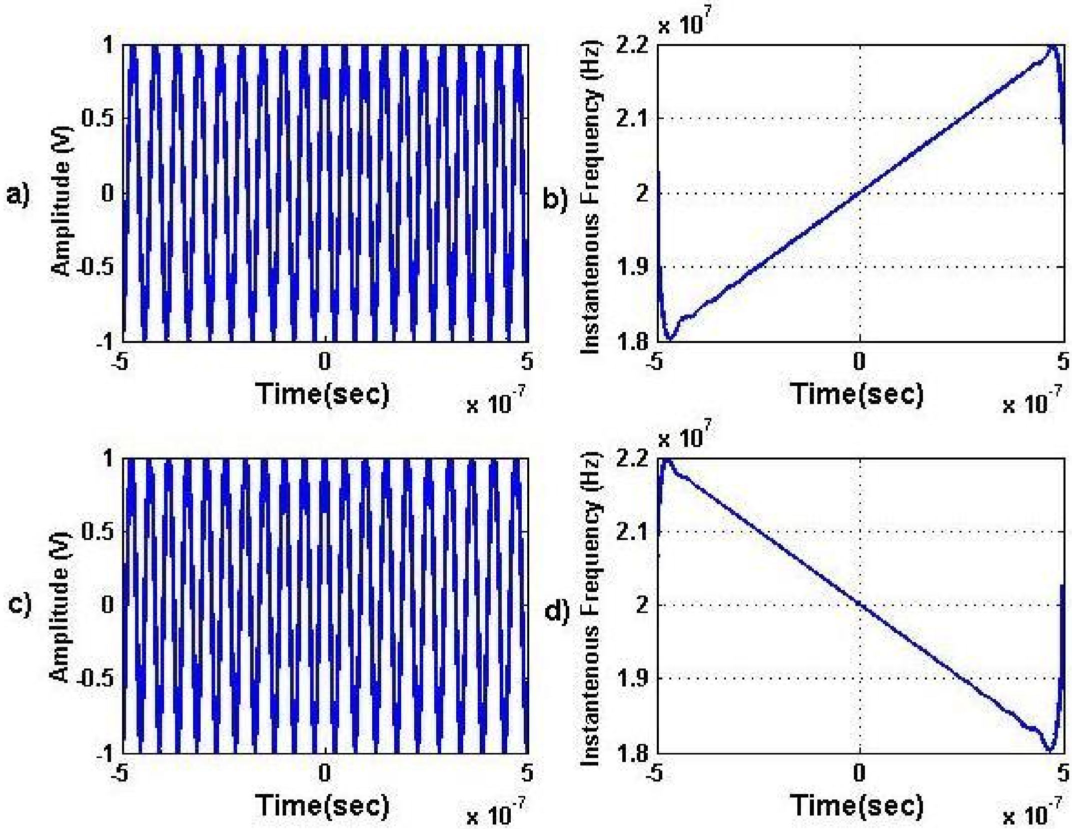

Figure 2.7 Chirp waveforms and instantenous frequencies: a) Up Chirp Signal b) Inst. Freq. of Up chirp signal, c) Down chirp signal, d) Inst Freq. of Down chirp signal

The parameters given in Eq. (2.6) are tuned to generate alternative digital modulated signals in CSS communication systems. The most common CSS signaling in digital communication systems are chirp binary orthogonal keying (Chirp-BOK) and antipodal chirp keying or chirp bipolar phase shift keying (Chirp-BPSK). In the next subsection, these techniques are briefly explained.

2.3 Chirp Spread Spectrum Communication System

2.3.1 Chirp-BOK Keying

This digital communication technique is primarily based on swithing the chirp rate according to the binary information. If data bit is logic “0”, the chirp signal having increasing instantaneous frequency, called as up-chirp is generated within a bit duration. If data bit is logic “1”, then, the chirp signal having decreasing instantaneous frequency, called as down-chirp is generated within a bit duration.

The transmitted signal waveform is mathematically expressed as in Eq. (2.10) (Springer et al., 2000).

$$s_{BOK}(t) = \begin{cases} A\,cos(2\pi f_c t + \pi\mu t^2) & "0" \textit{is transmitted} \\ A\,cos(2\pi f_c t - \pi\mu t^2) & "1" \textit{is transmitted}. \end{cases} \tag{2.10}$$

The illustration of sample Chirp-BOK keying is already given in Figure 2.7. It is important to check whether the up-chirp or down-chirp signal is properly designed according to the bandwidth limitation and has a constant envelope waveform having continuous linear instantaneous frequency.

In Chirp-BOK, each of chirp signals corresponds to only one bit to be transmitted. The low data rate can be increased by overlapping process to make it as possible as maximum. Thus, the transmitted pulse signal is compressed in time.

2.3.2 Antipodal Chirp Keying

Antipodal chirp-keying is based on generating chirp signals having opposite sign with respect to different binary message. If data bit is logic “0”, then the chirp signal having a specified chirp rate (up-chirp or down-chirp) is generated. If data bit is logic “1”, the phase of the chirp signal shifts to π and then, the amplitude of signal has the opposite sign (Haykin, 2001). The antipodal chirp waveform can be mathematically expressed as in Eq. (2.11)

$$s_{\mathrm{Antipodal}}(t) = \begin{cases} \mathrm{A}\cos(2\pi f_c t + \pi\mu t^2) & \text{"0" is transmitted} \\ \mathrm{A}\cos(2\pi f_c t + \pi\mu t^2 + \pi) & \text{"1" is transmitted.} \end{cases} \tag{2.11}$$

Antipodal chirp keying can be considered as Chirp-BPSK with zero chirp rate parameter. The sample waveform of antipodal chirp signal having the same signal specifications given in Section 2.2 are shown in Figure 2.8.

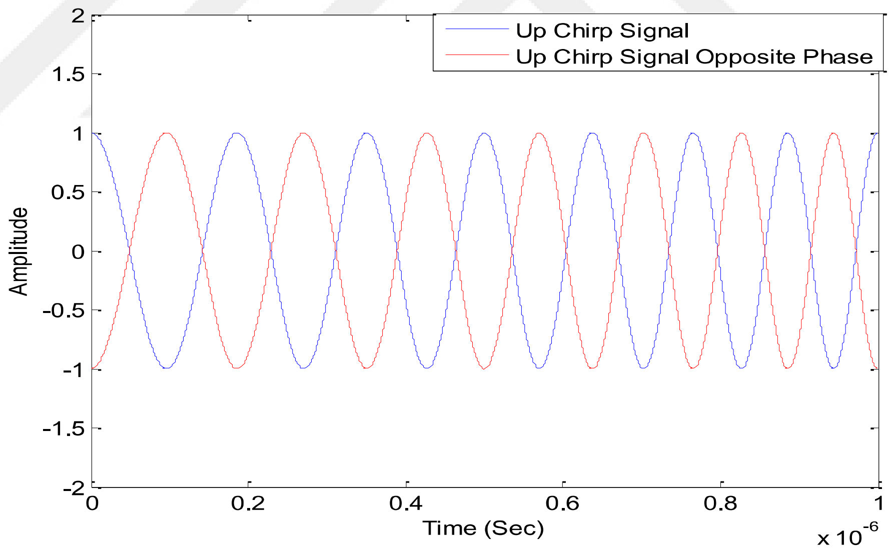

Figure 2.8 Antipodal chirp waveform

Once the chirp waveform $s(t)$ is constructed, then the impulse response corresponding to matched filter, is formulized as

$$\psi_{ss}(t) = h(t) * s(t) \tag{2.12}$$

where $\psi_{ss}(t)$ in Eq. (2.13) includes a *Sinc* function corresponding to $\sin(x)/x$ as the autocorrelation function of $s(t)$ expressed in Eq. (2.6) over bit interval for $-T_c < t < T_c$ and $h(t)$ characterizes the channel (Springer et al., 2000)

$$\psi_{ss}(t) = \sqrt{BT_c}\frac{\sin[\pi Bt(1-\frac{|t|}{T_c})]}{\pi Bt}\cos(2\pi f_c t) \tag{2.13}$$

where the bandwidth is given as $B = |\mu|T_c$. For two selected bandwidths and central frequency values, autocorrelation functions are plotted in Figure 2.9.

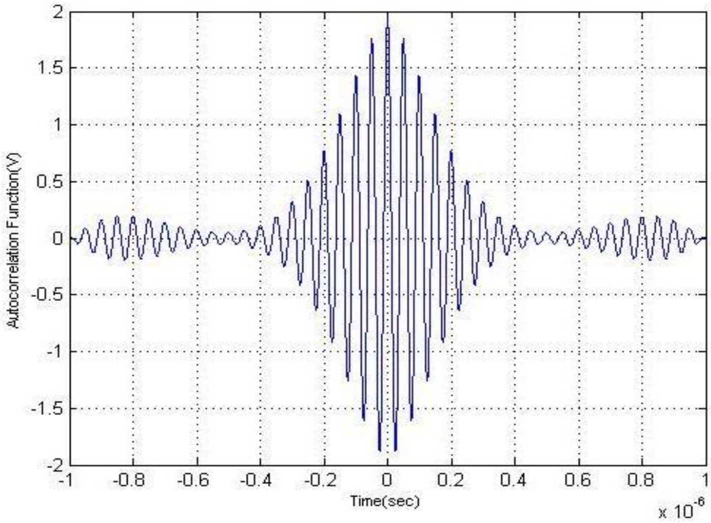

(a)

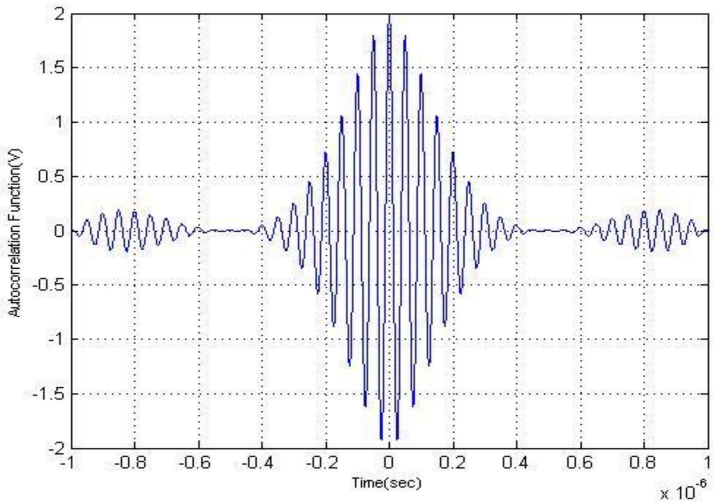

(b)

Figure 2.9 (a) Autocorrelation of chirp signal with respect to $f_c = 20\ MHz$ and $B = 3.8\ MHz$ and (b) $f_c = 20\ MHz$ and $B = 4\ MHz$

In Figure 2.9, a maximum peak of the amplitude of $\psi_{ss}(t)$ is derived as $\sqrt{BT_c}$ at $t = 0$. According to the illustration, its polar zeros are about $\pm 1/B$. For the selection of parameters either $B = 3.8\ MHz$ or $B = 4\ MHz$, $\psi_{ss}(t) = 2V$, but polar zeros vary with respect to changing of the bandwidth, B. The distance between polar zeros constitutes mainlobe width. Autocorrelation function of $s(t)$ corresponds to convolution to the impulse response with opposite sign of chirp rate of an ideal matched filter.

As described in Chirp-BOK keying subsection, the chirp signal is given as,

$$\begin{aligned} s_{BOK1}(t) &= A\cos(2\pi f_c t + \pi\mu t^2) \\ s_{BOK0}(t) &= A\cos(2\pi f_c t - \pi\mu t^2) \end{aligned} \tag{2.14}$$

where $A = \sqrt{\frac{2E_b}{T_c}}$ with bit energy E_b over a bit interval $-\frac{T_c}{2} < t < \frac{T_c}{2}$. The transmitted signal is represented as,

$$s(t) = \begin{Bmatrix} s_{BOK1}(t), & for\ \ b = 1 \\ s_{BOK0}(t), & for\ \ b = 0 \end{Bmatrix} \tag{2.15}$$

where b is binary symbol corresponding to the transmitted chirp signal. The energy of the transmitted signal is calculated as follows

$$E_b = \int_{-\frac{T_c}{2}}^{\frac{T_c}{2}} s^2(t)\, dt. \tag{2.16}$$

In AWGN channel with zero mean and variance $N_0/2$, the received signal is composed of transmitted signal and AWGN

$$r(t) = s(t) + n(t). \tag{2.17}$$

The noisy received signal is multiplied with up-chirp $s_{BOK1}(t)$ and down-chirp $s_{BOK0}(t)$ respectively, and thus, is low pass filtered by taking the integration of the locally chirp signal waveform over the same period. Finally, as represented in DSSS section, decision factor, u is as follows

$$u = \frac{1}{\sqrt{E_b}} \int_{-\frac{T_c}{2}}^{\frac{T_c}{2}} s(t) r(t)\, dt. \tag{2.18}$$

$r(t)$ is low-pass filtered over $-\frac{T_c}{2} \leq t \leq \frac{T_c}{2}$ and the term $s(t) * n(t)$ is neglected to correlate the information-bearing data bits properly. Decision factor, u, is calculated and compared with the threshold. A decision is made whether the binary symbol is '1' or '0' with respect to the threshold level. For Chirp-BOK, theoretical BER is given by (Springer et al., 2000)

$$P_e = \frac{1}{2} erfc\left(\sqrt{E_b / 4N_0}\right). \tag{2.19}$$

The block diagrams of Chirp-BOK and Antipodal Chirp keying communication systems are shown by Figure 2.10 and Figure 2.11, respectively.

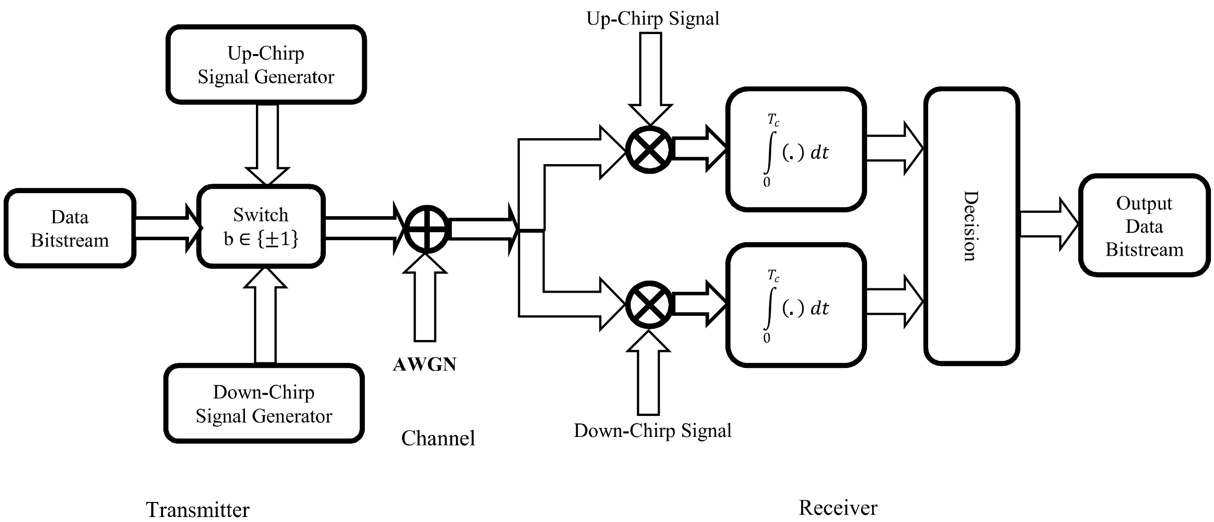

Figure 2.10 Block diagram of Chirp-BOK system with AWGN

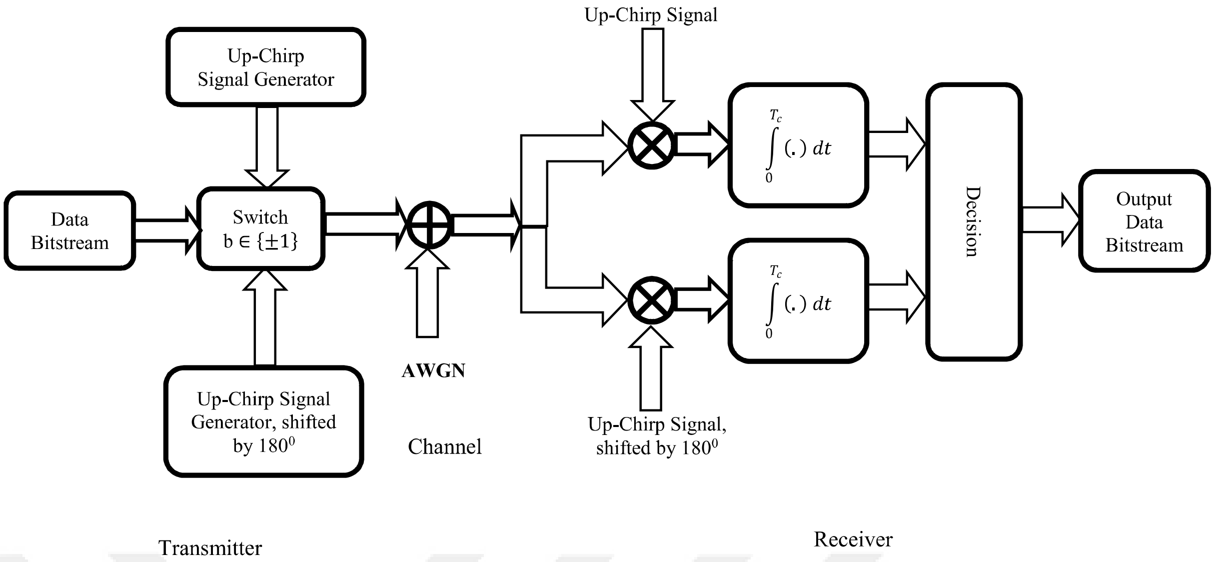

Figure 2.11 Block diagram of Antipodal Chirp system with AWGN

In Antipodal Chirp Keying as BPSK scheme, the phase of $s(t)$ is shifted by 180 degrees with respect to bit symbols. Thus, the polarity of amplitude, A, is $-\sqrt{\frac{2E_b}{T_b}}$, and has an opposite sign for $s_{\text{Antipodal\_0}}(t)$. Autocorrelation function of the antipodal chirp signal also appears the same as that of Chirp-BOK in the compressed pulse. The receiver determines the sign of the matched filter output with respect to the reference signal having no phase shift, assuming coherent detection. The error performance of this communication system is expressed as the average probability of error of BPSK modulation in AWGN which is given as

$$P_e = Q\left(\left(\sqrt{{2E_b}/{N_0}}\right)\right) = \frac{1}{2}erfc\left(\sqrt{{E_b}/{N_0}}\right) \tag{2.20}$$

where $erfc$ is the complementary error function.

To validate simulation results in MATLAB, the experiment computes 50000 data bit running at each SNR value for AWGN case and, is then repeated by 10 times. If SNR is represented by $EsNo$, the relation between $EsNo$ and $EbNo$ formulized as in Eq. (2.21)

$$EsNo\ (dB) = EbNo\ (dB) + 10 * log_{10}(k) \tag{2.21}$$

by using the term, $k = \log_2 M$ where k is the number of bits per symbol and M refers to M-ary communication. SNR is also equivalently represented in terms of $EbNo$, depending on bit rate R_b (in bits/sec) and sampling frequency F_s used in simulation, as given in Eq. (2.22).

$$SNR\ (dB) = -3\ (dB) + \log_{10}\left(\frac{F_s}{R_b}\right) + EbNo\ (dB) \tag{2.22}$$

where $R_b = 1\ Mb/sec$ in the simulations. Finally, the BER performances of both CSS systems in AWGN channel environment is shown in Figure 2.12 and 2.13.

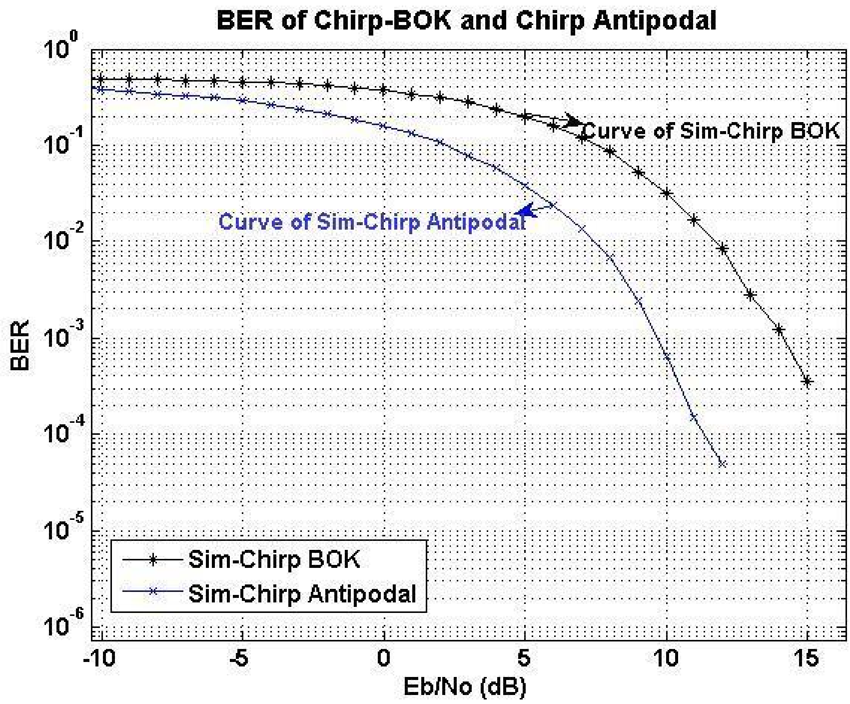

Figure 2.12 Simulation BER results of Chirp-BOK compared with simulation BER results of Chirp-Antipodal

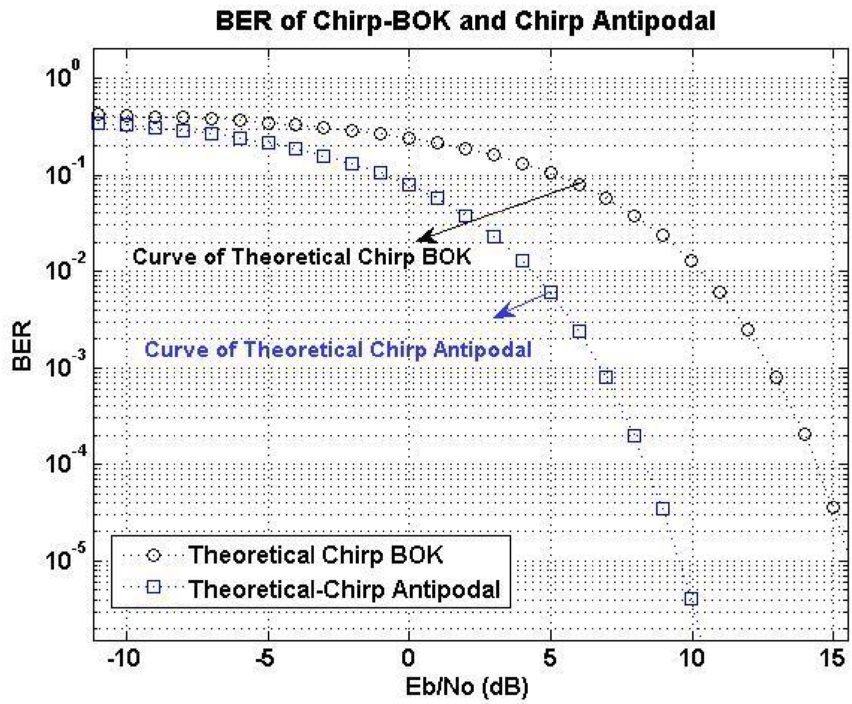

Figure 2.13 Theoretical BER results of Chirp-BOK compared with theoretical BER results of Chirp-Antipodal

In the simulations, the symbol duration and sampling frequency are taken as $T_c = 1\,\mu$ and $F_s = 500\,MHz$ for 10000 message bits and 10 realizations due to the computational restrictions. It can be concluded that there is slight difference between theoretical and simulation result since the number of message bits and realizations cannot sufficiently ensure the convergence of BER to theoretical values.

On the other hand, one can see that antipodal chirp modulation based communication system exhibits superior performance compared with chirp-BOK keying since the chirp-BOK signals with respect to message bits “0” and “1” are not completely orthogonal whereas there is an apparent correlation difference for the signal assigned for complement message bit.

CHAPTER THREE
RECEIVER TYPES IN α-STABLE NOISE CHANNELS

In digital communication, the additive noise in the channel discarding the multipath effects is commonly assumed to be Gaussian. But in practical situations, the probability distribution of the noise may exhibit non-Gaussian, especially impulsive behavior. Therefore, alternative densities are utilized to formulize the distribution of the channel noise. The proper candidate to model the non-Gaussian noise is α-stable distributions. This chapter is primarily based on describing α-stable distributions and detecting signals in stable noise environment. In the sequel, α-stable distribution and its properties are briefly described.

3.1 α-Stable Distributions

α-stable distributions can be considered as a family of distributions having the properties of skewness and heavy tailness. Among the several formal description of definition, α-stable distribution can be defined as follows.

3.1.1 Definition of α-Stable Distributions

A random variable X is said to have a stable distribution if for any positive real numbers A and B, there are positive real numbers C and D such that

$$AX_1 + BX_2 \stackrel{\text{def}}{=} CX + D \tag{3.1}$$

where X_1 and X_2 are independent realizations of X and the term "$\stackrel{\text{def}}{=}$" denotes equality in distribution (Samorodnitsky, 1994).

One dimensional α-stable distribution of a random variable X is described by its characteristic function as given below (Samorodnitsky, 1994)

$$\varphi(\omega) = \begin{cases} exp\left\{-\sigma^{\alpha}|\omega|^{\alpha}\left(1 - j\beta\big(sign(\omega)\big)\tan\frac{\pi\alpha}{2}\right) + j\eta\omega\right\} & if\ \alpha \neq 1 \\ exp\left\{-\sigma|\omega|\left(1 + j\beta\frac{2}{\pi}\big(sign(\omega)\big)\ln|\omega|\right) + j\eta\omega\right\} & if\ \alpha = 1 \end{cases} \quad (3.2)$$

where the function $sign(\omega)$ is defined as $sign(\omega) = \begin{cases} 1 & if\ \omega > 0 \\ 0 & if\ \omega = 0. \\ -1 & if\ \omega < 0 \end{cases}$

In Eq. (3.2), characteristic exponent α, skewness parameter β, scale parameter σ or in other words the equivalent dispersion parameter $\gamma = \sigma^{\alpha}$, and finally the location parameter η, tune impulsiveness, asymmetry, intensity, and the amount of shift, respectively. The probability density function can be obtained from its characteristic function as (Janicki & Weron, 1994)

$$f(x) = \frac{1}{2\pi}\int_{-\infty}^{\infty}\varphi(\omega)\, e^{-j\omega x}d\omega. \quad (3.3)$$

In order to verify the notation, α-stable distributed random variable can be represented by $X \sim S_{\alpha}(\sigma, \beta, \eta)$. However, the probability density function (pdf) of α-stable distributions can not be determined analytically. (Janicki & Weron, 1994) stated exceptional cases which are, Gaussian distribution represented by $S_2(\sigma, 0, \eta)$

$$f(x) = \frac{exp\{-(x-\eta)^2/4\sigma^2\}}{2\sigma\sqrt{\pi}} \quad (3.4)$$

Cauchy distribution represented by $S_1(\sigma, 0, \eta)$

$$f(x) = \frac{2\sigma}{\pi((x-\eta)^2 + 4\sigma^2)} \quad (3.5)$$

and Levy distribution represented by $S_{1/2}(\sigma, 1, \eta)$

$$f(x) = \left(\frac{\sigma}{2\pi}\right)^{\frac{1}{2}}(x-\eta)^{-\frac{3}{2}}\mathrm{e}^{\left(-\frac{\sigma}{2(x-\eta)}\right)} \quad (3.6)$$

where $f(x) = 0$ for $x \in (-\infty, \eta)$. The effect of the parameters on pdfs are plotted in the sequel. The effect of characteristic exponent is shown in Figure 3.1. It can be seen that the area under the tails of the distribution increases when the impulsiveness of the noise increases i.e., α decreases.

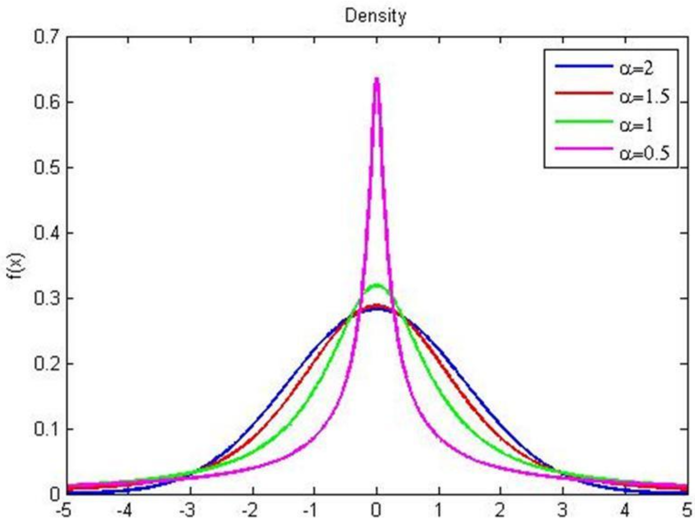

Figure 3.1 Pdfs with respect to various α values where $\beta = 0, \sigma = 1, \eta = 0$

The effect of skewness is illustrated in Figure 3.2. When the skewness is positive, the area under the pdf function is mostly on the positive side and the opposite is same for negative skewness.

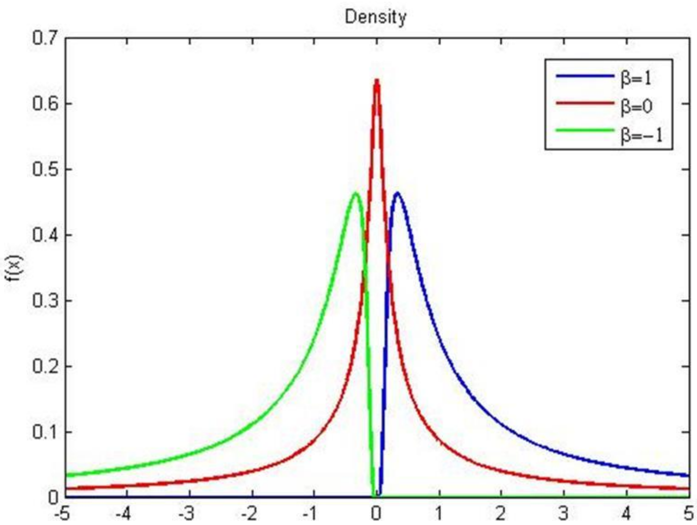

Figure 3.2 Pdfs with respect to various β values where $\alpha = 0.5, \sigma = 1, \eta = 0$

Finally, the effect of scale parameter is shown in Figure 3.3.

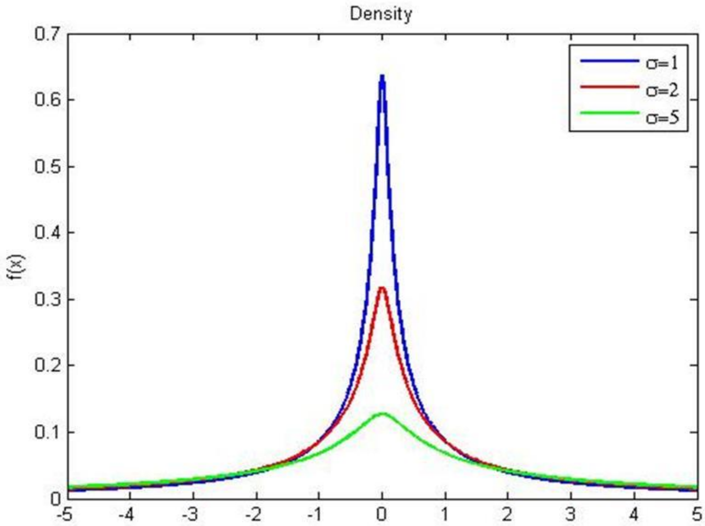

Figure 3.3 Pdfs with respect to various σ values where $\alpha = 0.5, \beta = 0, \eta = 0$

3.1.2 Properties of α-Stable Distributions

In this section, some properties of α-stable distributions comprehensively given by (Samorodnitsky & Taqqu, 1994) are briefly summarized as follows.

Property 3.1.2.1 Let X_1 and X_2 be independent random variables with $X_i \sim S_\alpha(\sigma_i, \beta_i, \eta_i)$, i=1,2. Then $X_1 + X_2 \sim S_\alpha(\sigma, \beta, \eta)$, with

$$\sigma = (\sigma_1^\alpha + \sigma_2^\alpha)^{1/\alpha}, \beta = \frac{\beta_1\sigma_1^\alpha + \beta_2\sigma_2^\alpha}{\sigma_1^\alpha + \sigma_2^\alpha}, \eta = \eta_1 + \eta_2.$$

Property 3.1.2.2 Let $X \sim S_\alpha(\sigma, \beta, \eta)$ and a be a real constant. Then,

$$X + a \sim S_\alpha(\sigma, \beta, \eta + a).$$

Property 3.1.2.3 Let $X \sim S_\alpha(\sigma, \beta, \eta)$ and let a be a non-zero real constant. Then

$$aX \sim S_\alpha(|a|\sigma, sign(a)\beta, a\eta) \qquad if\ \alpha \neq 1$$
$$aX \sim S_1\left(|a|\sigma, sign(a)\beta, a\eta - \frac{2}{\pi}a(\ln|a|)\sigma\beta\right) \qquad if\ \alpha = 1.$$

Property 3.1.2.4 For any $0 < \alpha < 2$,

$$X \sim S_\alpha(\sigma, \beta, 0) \Leftrightarrow -X \sim S_\alpha(\sigma, -\beta, 0).$$

Property 3.1.2.5 $X \sim S_\alpha(\sigma, \beta, \eta)$ is symmetric if and only if $\beta = 0$ and $\eta = 0$. It is symmetric about η if and only if $\beta = 0$.

Property 3.1.2.6 Let $X \sim S_\alpha(\sigma, \beta, \eta)$ with $\alpha \neq 1$. Then X is strictly stable if and only if $\eta = 0$.

Property 3.1.2.7 Let $X \sim S_\alpha(\sigma, \beta, \eta)$ with $0 < \alpha < 2$. Then

$$\begin{aligned} E|X|^p &< \infty \qquad for\ any\ 0 < p < \alpha \\ E|X|^p &= \infty \qquad for\ any\ p \geq \alpha. \end{aligned}$$

Property 3.1.2.8 Let $X \sim S_\alpha(\sigma, \beta, 0)$ with $0 < \alpha < 2$ and $\beta = 0$ in the case $\alpha = 1$. Then, for every $0 < p < \alpha$, there is a constant $c_{\alpha,\beta}(p)$ such that

$$(E|X|^p)^{1/p} = c_{\alpha,\beta}(p)\sigma.$$

The constant $c_{\alpha,\beta}(p)$ equals $(E|X_0|^p)^{1/p}$ where $X_0 \sim S_\alpha(1, \beta, 0)$.

3.2 BER Analysis For Several Digital Modulation Schemes Under Symmetric α-Stable Noise

Among several studies related with analysis of signal detection problem in alpha-stable noise using several modulation techniques, (Yang & Zhang, 2014) had remarkable study in order to extract approximately analytical bit error rate expression.

According to this study, consider that *U* is assumed to be a logarithmic-order random variable. The geometric power of *U* is defined as

$$S_0 = S_0(U) \triangleq exp(\mathbb{E}[log|U|]) = \gamma_s C_g^{\left(\frac{1}{\alpha}-1\right)} \tag{3.7}$$

where $\mathbb{E}(.)$ denotes expectation operator, C_g is the exponential Euler constant and equals approximately $C_g \approx 1.78$. The GSNR Υ_G designed in case of Gaussian for $\alpha = 2$ can be expressed as

$$\Upsilon_G = \frac{A^2}{2C_g(S_0)^2} = \frac{A^2}{2C_g^{\left(\frac{2}{\alpha}-1\right)}\gamma_s^2} \tag{3.8}$$

where A is the root mean square (RMS) amplitude of the transmitted signal. Because the real and imaginary components are assumed to be independent $S\alpha S$ variables, each has an average power $N_0/2$ in case of $\alpha = 2$ (Yang & Zhang, 2014).

Then, we obtain

$$E_b/N_o = \frac{\Upsilon_G}{2} = \frac{A^2}{4C_g^{\left(\frac{2}{\alpha}-1\right)}\gamma_s^2} \tag{3.9}$$

where E_b is the signal energy per symbol (Yang & Zhang, 2014).

A random variable Y follows Gaussian distribution with mean μ and variance σ^2 can be represented as $Y \sim \mathcal{N}(\mu, \sigma^2)$. The pdf of Gaussian distribution is given by

$$g(y) = \frac{1}{\sigma\sqrt{2\pi}} exp\left(-\frac{(y-\eta)^2}{2\sigma^2}\right). \tag{3.10}$$

The normal distribution with $\eta = 0$ and $\sigma^2 = 1$ is converted to derive a standard normal distribution. The standardized process for a normal distributed variable Y is implemented by changing Y to $Z = (Y - \eta)/\sigma$, i.e., $Z \sim \mathcal{N}(0,1)$, yielding

$$g(y)dy = g_0(z)dz, \tag{3.11}$$

where $g(y)$ is given in Eq. (3.11), and $g_0(z)$ is the pdf of standard normal distribution represented as

$$g_0(z) = \frac{1}{\sqrt{2\pi}} exp\left(-\frac{z^2}{2}\right). \tag{3.12}$$

If random variable U is given as the general $S\alpha S$ distribution with $U \sim S(\alpha, 0, \gamma_s, 0)$, then $V = \frac{U}{\gamma_s}$ transforms as standard $S\alpha S$ distribution, i.e., $V \sim S(\alpha, 0,1,0)$ (Yang & Zhang, 2014).

The standardized process for general $S\alpha S$ distributed variable yields

$$f(u; \alpha)du = f_0(v; \alpha)dv, \qquad \alpha \in (0,2]. \tag{3.13}$$

where $f(u; \alpha)$ is shown in Eq. (3.13), and $f_0(v; \alpha)$ is the pdf of standard $S\alpha S$ distribution defined by setting $\gamma_g = 1$ in Eq. (3.14),

$$f_0(v; \alpha) \triangleq \frac{1}{\pi} \int_0^{+\infty} exp(-|\omega|^\alpha) \cos(v\omega)\, d\omega, \qquad \alpha \in (0,2]. \tag{3.14}$$

Noting that the Q-function is defined in Eq. (3.15),

$$Q(x) \triangleq \frac{1}{\sqrt{2\pi}} \int_x^{+\infty} exp\left(-\frac{z^2}{2}\right) dz = \int_x^{+\infty} g_0(z)dz, \tag{3.15}$$

the tail probability function for $S\alpha S$ distribution with value α as (Yang & Zhang, 2014) is described as follows

$$Q_s(x; \alpha) \triangleq \int_x^{+\infty} f_0(v; \alpha)dv = \frac{1}{\pi} \int_x^{+\infty} \int_0^{+\infty} exp(-|\omega|^\alpha) \cos(v\omega)\, d\omega dv. \tag{3.16}$$

3.3 Several Receiver Types For Signal Detection in Gaussian and α -Stable Interference

The detection performance in wireless communication systems gets worse in presence of α-stable distributed interference, which may be recorded by wireless sensors in or around jet engines, and caused by large metallic rotating objects, large electromechanical systems, and aircraft communication equipment, compared to AWGN noise (Kadri et al., 2011).

The received signal $y[n]$ sampled at N points within having symbol duration T_b according to the basic two chirp modulation types formulated as

$$s_i[n] = \begin{cases} s_{BOK1}[n] & if\ i = 1 \\ s_{BOK0}[n] & if\ i = 0 \end{cases} \quad for\ chirp\ BOK\ and$$

$$s_i[n] = \begin{cases} s_{Antipodal1}[n] & if\ i = 1 \\ s_{Antipodal0}[n] & if\ i = 0 \end{cases} \quad for\ chirp\ antipodal\ or\ BPSK. \tag{3.17}$$

Noise only modelled as AWGN can be detected by optimum receivers. In more general case, α-stable interference can be considered together with Gaussian noise in communication channel. The total noise signal is formulized as

$$v = n_s + n_g \tag{3.18}$$

where n_s is a $S\alpha S$ distributed random variable, $n_s \sim S_\alpha(\gamma_s, 0, 0)$ and n_g is a Gaussian random variable, $n_g \sim N(0, \sigma_g^2)$ with variance $\sigma_g^2 = 2\gamma_g$ and zero-mean. n_s and n_g are assumed to be independent random variables. Then, the characteristic functions of two independent random variables are multiplied with each other. The resultant characteristic function of the sum of these two random variables in Eq. (3.19) may now be written as

$$\varphi_V(\omega) = \varphi_s(\omega)\varphi_g(\omega) = e^{-\gamma_s|\omega|^\alpha} e^{-\gamma_g \omega^2}. \tag{3.19}$$

Thus, the pdf of noise by replacing in Eq. (3.3), may now be written as

$$f_v(v) = f(v;\alpha) = \frac{1}{\pi}\int_0^{\infty} e^{-\gamma_s|\omega|^{\alpha}} e^{-\gamma_g \omega^2} \cos(\omega v)\, d\omega. \tag{3.20}$$

This interference was analyzed in the literature for the case of $\alpha \in \{1,2\}$ in α-stable distribution properties. The main disadvantage in presence of both stable and Gaussian noise is the non-existence of solution in closed form. To be detected by optimum receivers becomes too hard. Instead of optimum receivers, several sub-optimum receivers have been developed recently. Under normal circumstances, since α, γ_s, and γ_g parameters cannot be known in advance and, estimation of these parameters in α-stable noise is crucial. Although different types of estimators such as Pickands estimator, Hill estimator, De Haan and Resnick estimator and fractional order moment estimator are used, empirical characteristic function (ECF) with the stronger performance is more suitable for α-stable noise (Sureka et al., 2013).

Since the BER of a communication system can be measured by signal-to-noise ratio (SNR), the noise variance is estimated by using second-order statistics. Whereas, the alpha-stable noise with $\alpha < 2$ has infinite variance geometric signal-to-noise power ratio (GSNR) defined by geometric power is a suitable tool for $S\alpha S$ noise measurement (Sureka et al., 2013). The generalized signal-to-noise ratio can be given as in Eq. (3.21),

$$GSNR = 10\, log_{10}\left(\frac{\sum_{n=1}^{N} s_i^2[n]}{N(\gamma_s+\gamma_g)}\right). \tag{3.21}$$

Then, the received signal is

$$y[n] = s_i[n] + v[n], \quad i \in \{0,1\},\ n \in \{1,2,\ldots,N\} \tag{3.22}$$

where $v[n]$ is the noise signal (considered as i.i.d. random variable) from the noise model defined in Eq. (3.3). The signals $s_i[n]$ are also assumed to have equal prior probabilities. In this case, detection problem can be solved by defining binary hypothesis test as follows

$$\begin{aligned} H_0: y[n] &= s_0[n] + v[n], \qquad n \in \{1,2,\ldots,N\}, \\ H_1: y[n] &= s_1[n] + v[n], \qquad n \in \{1,2,\ldots,N\}. \end{aligned} \tag{3.23}$$

However, being several receiver types we examine two possible receiver structures such as the Linear AWGN receiver, the Cauchy receiver. The test statistic for each of these cases is given below (Sureka et al., 2013).

- Linear AWGN receiver: Compared with $s_i[n]$, the test stastistic for the received signal $y[n]$ sampled at N times in linear AWGN receiver is

$$\Lambda_L = \sum_{n=1}^{N} y[n]\, s_0[n] \underset{\mathcal{H}_1}{\overset{\mathcal{H}_0}{\gtrless}} 0 \tag{3.24}$$

- Cauchy receiver: Cauchy pdf with a closed-form $S\alpha S$ distribution is as follows

$$f_{Cauchy}(v) = \frac{\gamma_s}{\pi(\gamma_s{}^2 + |v|^2)} \tag{3.25}$$

By taking logarithm of the ratio of Cauchy pdfs, with respect to binary hypothesis testing problem given in Eq. (3.23), the test stastistic is obtained as

$$\Lambda_C = \sum_{n=1}^{N} \log \frac{f_{Cauchy}(y[n]-s_0[n])}{f_{Cauchy}(y[n]-s_1[n])} \underset{\mathcal{H}_1}{\overset{\mathcal{H}_0}{\gtrless}} 0. \tag{3.26}$$

The error performances of Chirp BOK keying and Antipodal Chirp keying given according to the absence of Gaussian distribution ($\gamma_G = 0$) are shown in Figure 3.4 and Figure 3.5 according to the characteristic exponent $\alpha = 1.8$ and $\alpha = 1.6$, respectively. BER results are illustrated with respect to GSNR for 5000 bits of data and 10 realizations for linear receiver.

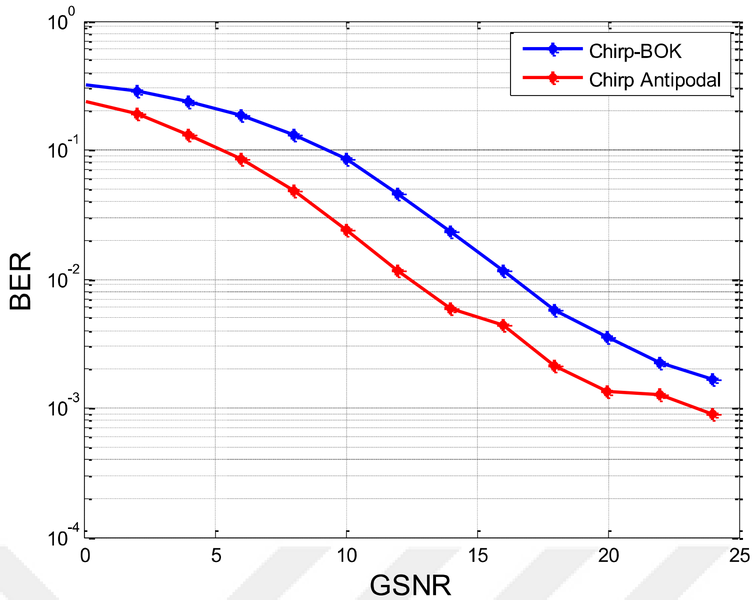

Figure 3.4 BER performance of Chirp modulation systems under $S\alpha S$ noise. $\alpha = 1.8, \beta = 0$

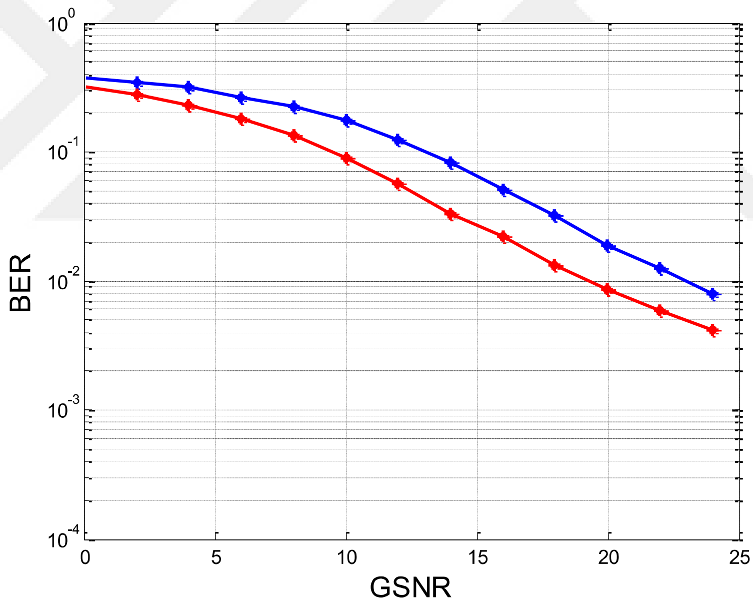

Figure 3.5 BER performance of Chirp modulation systems under $S\alpha S$ noise. $\alpha = 1.6, \beta = 0$

One can conclude that there is certain gap between BER performances of Chirp – BOK keying and Chirp Antipodal Keying and antipodal signaling yields superior performance under impulsive noise. On the other hand, the effect of characteristic exponent is represented for both modulation techniques in Figure 3.6 and Figure 3.7, respectively.

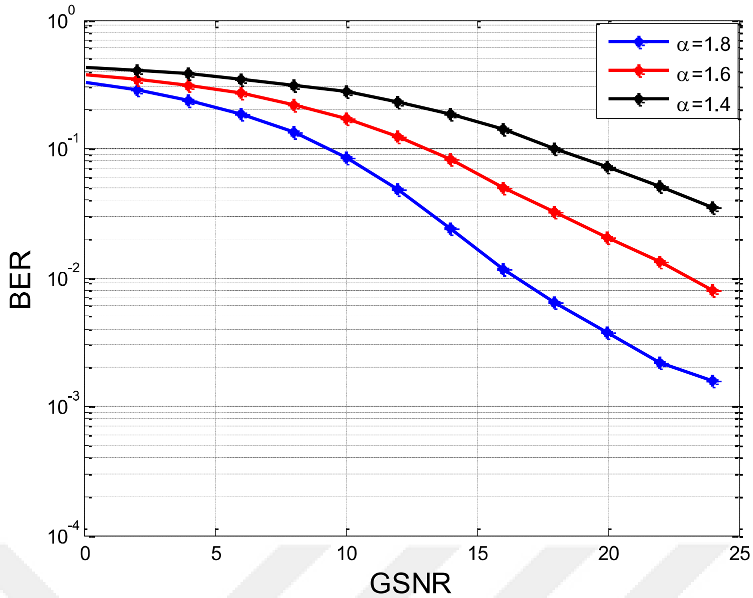

Figure 3.6 BER performance of Chirp BOK keying communication with respect to various characteristic exponent values for linear receiver

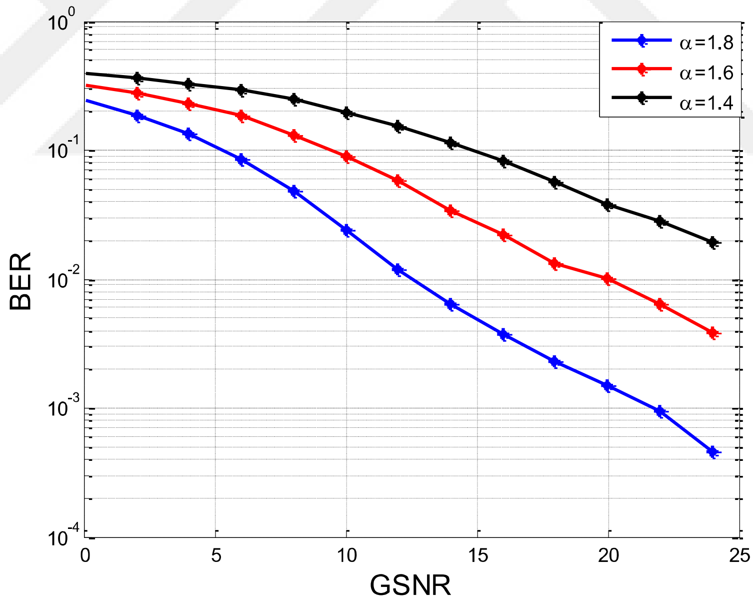

Figure 3.7 BER performance of Chirp Antipodal keying communication with respect to various characteristic exponent values for linear receiver

It is obvious for both chirp modulation types, the error performances degrade when the impulsiveness of the channel increases, i.e., α decreases.

The second receiver described by Eq. (3.26) is the Cauchy receiver which utilizes the Cauchy distribution given by Eq. (3.25). The test statistics obtained by Eq. (3.26) is used to evaluate the error performance of the Cauchy receiver. Similarly, the BER performances with respect to Chirp BOK keying and Chirp Antipodal keying systems are shown in Figure 3.8 and Figure 3.9 for $\alpha = 1.8$ and $\alpha = 1.6$, respectively.

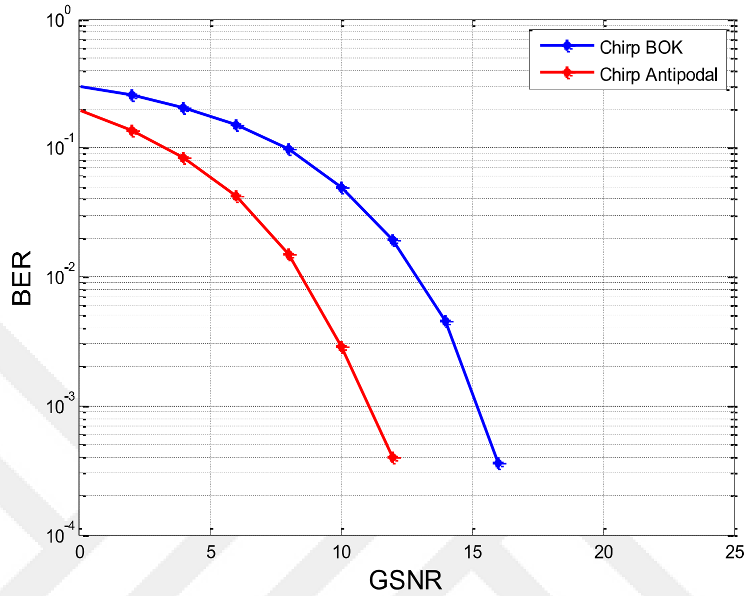

Figure 3.8 BER performance of Cauchy receiver based Chirp modulation systems under $S\alpha S$ noise. $\alpha = 1.8, \beta = 0$

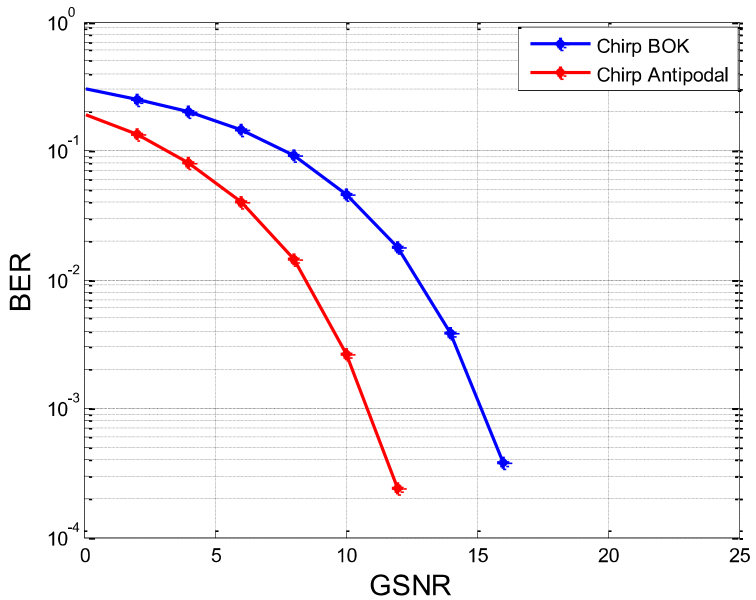

Figure 3.9 BER performance of Cauchy receiver based Chirp modulation systems under $S\alpha S$ noise. $\alpha = 1.6, \beta = 0$

It is observed that the error performance of Chirp Antipodal keying is better than Chirp-BOK keying. Moreover, it can also be said that the Cauchy receiver performs better error rate result compared with linear receiver.

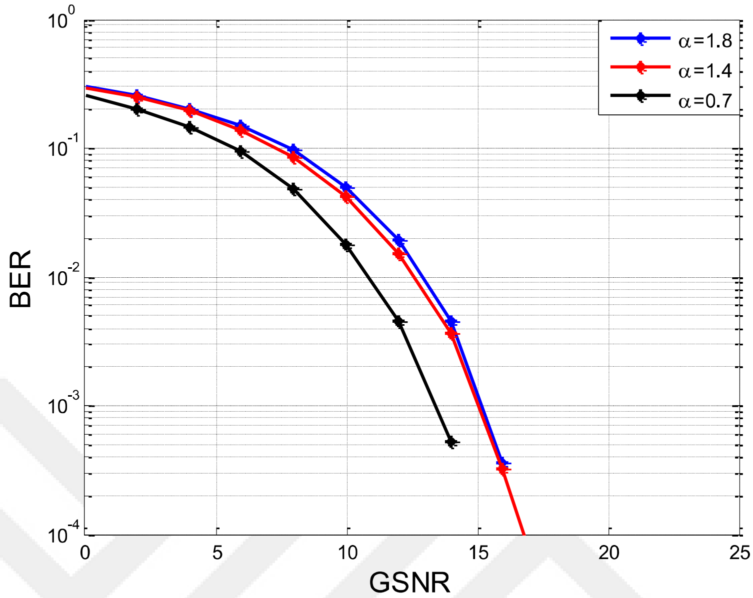

Figure 3.10 BER performance of Chirp BOK keying communication with respect to various characteristic exponent values for Cauchy receiver

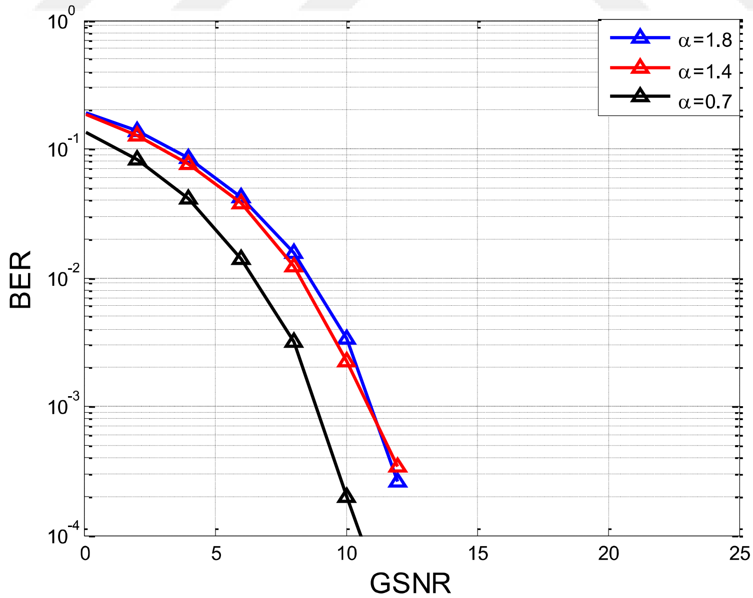

Figure 3.11 BER performance of Chirp Antipodal keying communication with respect to various characteristic exponent values for Cauchy receiver

The variation of error rate of the Chirp-BOK keying and Chirp Antipodal keying systems with respect to different characteristic exponents are illustrated in Figure 3.10 and Figure 3.11, respectively. Unlike the expectations, the Cauchy receiver exhibits almost same error performances when $1 < \alpha < 2$ and the error performance becomes apparently better when the impulsiveness increases.

Another study in the thesis is the simulation of error rate in presence of both $S\alpha S$ and Gaussian noise. The BER results of both modulation types for various characteristic exponents are shown in Figure 3.12 and Figure 3.13, utilizing Cauchy receiver and linear receiver, respectively.

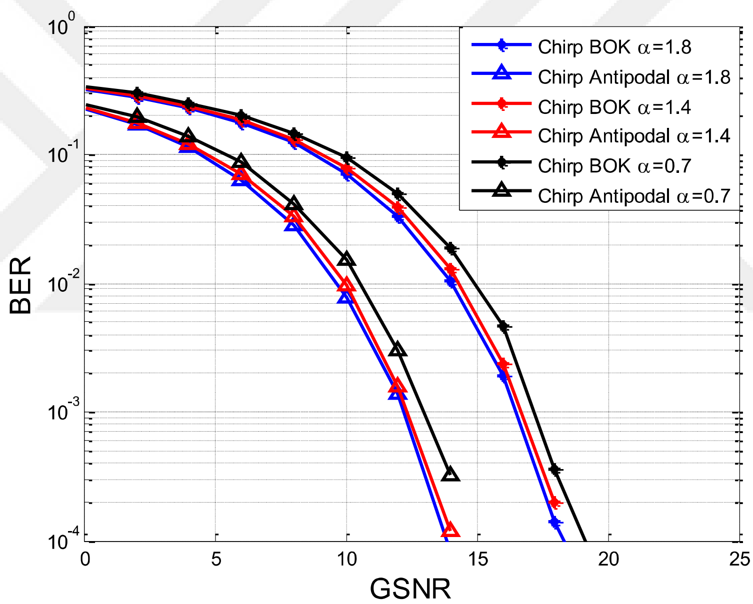

Figure 3.12 BER performance of Chirp-BOK and Chirp Antipodal keying communication systems in presence of both $S\alpha S$ and Gaussian noise with respect to various characteristic exponent values for Cauchy receiver

It can be concluded that the error performance slightly gets worse when the impulsiveness of the channel increases for both Cauchy and linear receivers. There is an apparent performance gap between the receivers observed by Figure 3.12 and Figure 3.13.

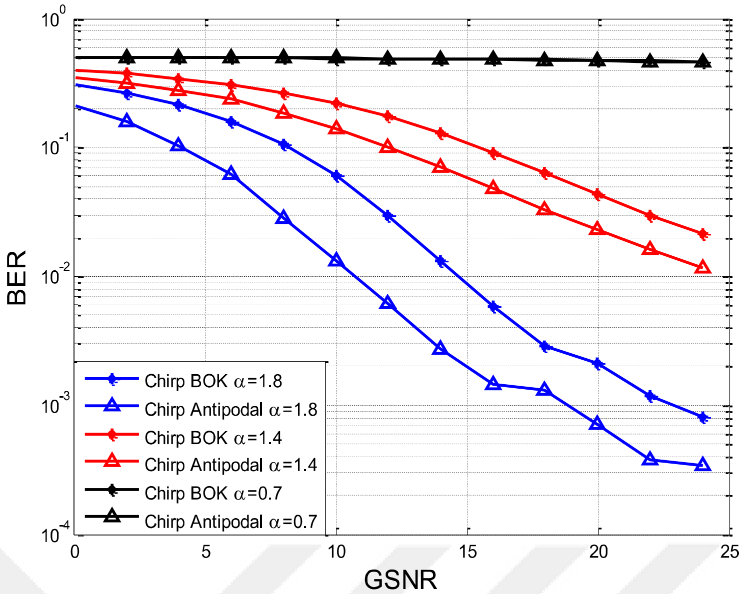

Figure 3.13 BER performance of Chirp-BOK and Chirp Antipodal keying communication systems in presence of both $S\alpha S$ and Gaussian noise with respect to various characteristic exponent values for Linear receiver

Besides, one can note that according to Figure 3.13, linear receiver cannot provide an error performance for $\alpha = 0.7$, since sample mean corresponds to first order moment and is not finite $\alpha < 1$. Also note that the Gaussian and stable noise intensities are taken to be equal while determining GSNR value.

CHAPTER FOUR
CONCLUSION

In this thesis, the chirp spread spectrum technique and basic chirp modulation based digital communication techniques are analyzed in the presence of $S\alpha S$ and/or Gaussian noise environment. The reason of analyzing chirp signal relies on the some properties due to applicability in wide variety of signal processing topics and also the potential robustness aspect against interference.

However, there are only a few studies on the performance of linear frequency modulated signals in $S\alpha S$ noise channels. With this motivation, the two basic chirp signaling techniques utilized in digital communication are performed under both Gaussian and stable noise, and under only stable noise. The BER performances are shown to indicate that, increasing impulsiveness directly increases the error rate. The conventional parameters affecting the overall communication system performance are selection of bandwidth, bit rate, and chirp rate.

It is observed that Cauchy receiver has a certain BER performance improvement compared with linear receiver under impulsive noise. On the other hand, Chirp-Antipodal keying gives promising results in presence of $S\alpha S$ noise. The Gaussian noise and impulsive noise are observed to decrease the error performances of both receivers.

In the future, novel receivers can be designed utilizing the properties of chirp signals to obtain better error performance for not only additive Gaussian and/or non-Gaussian noise but also multipath fading channel models.

REFERENCES

Bai, Z., Li, X., Yuan, D. & Kwak, K. (2012). Non-linear chirp based uwb waveform design for suppression of nbi. *Wireless Communications and Mobile Computing, 12*(6), 545-552.

Billa, R., Sharma, P. & Ashraf, J. (2012). Analysis of chirp spread spectrum system for multiple access. *International Journal of Engineering Research & Technology, 1*(3), 1-9.

Cong-ren, L, Hui-min, W. & Fei, Y. (2013). An improved modulation based on bok in underwater acoustic channel. *Advances in Information Sciences and Service Sciences 5, 5*, 396-402.

Djuric, P.M. & Kay, S.M. (1990). Parameter estimation of chirp signals. *IEEE Transactions on Acoustics, Speech and Signal Processing, 38*(12), 2118-2126.

Dotli´c, I. & Kohno, R. (2011). Low complexity chirp pulsed ultra wideband system with near-optimum multi-path performance. *IEEE Transactions on Wireless Communications 10*(1), 208-218.

Fanyu, M. & Xuemai, G. (2011). A combined chirp spread modulation technique for multiple access system. *Information Technology Journal, 10*, 416-421.

Guo, J., Zou, H., Yang, X. & Liu, G. (2011). Parameter estimation of multicomponent chirp signals via sparse representation. *IEEE Transactions on Aerospace and Electronic Systems, 47*(3), 2261-2268.

He, C., Ran, M., Meng, Q. & Huang, J. (2010). Underwater acoustic communications using m-ary chirp-dpsk modulation. *IEEE 10th International Conference on Signal Processing (ICSP)*, 1544-1547.

Hengstler, S., Kasilingam, D.P. & Costa, A.H. (2002). A novel chirp modulation spread spectrum technique for multiple access. *2002 IEEE Seventh International Symposium on Spread Spectrum Techniques and Applications, 1*, 73-77.

Huang, J., He, C. & Zhang, Q. (2005). M-ary chirp spread spectrum modulation for underwater acoustic communication. *TENCON 2005 2005 IEEE Region 10*, 1-4.

Janicki, A. & Weron, A. (1994). Simulation and chaotic behavior of α-stable stochastic processes. New York: Marcel Dekker,Inc.

Kadri, A., Rao, R.K. & Jiang, J. (2011). Detection and performance of weak m-ary chirp signals in class-a impulsive noise. *Wireless Communications and Networking Conference (WCNC), 2011 IEEE*, 1511-1516.

Kadri, A. (2012). Non-coherent detection of weak m-ary chirp signals in non-Gaussian impulsive noise. *8th International Wireless Communications and Mobile Computing Conference (IWCMC)*, 1180-1184.

Khan, M.A., Rao, R.K. & Wang, X. (2013). Closed form error probability for m-ary chirp modulation in frequency -selective and -nonselective fading channels. *26th Annual IEEE Canadian Conference on Electrical and Computer Engineering (CCECE)*, 1-4.

Lakshminarayana, H.K., Bhat, J.S., Jagadale, B.N. & Mahesh, H.M. (2009). Improved chirp modulation spread spectrum receiver based on fractional fourier transform for multiple access. *2009 International Conference on Signal Processing Systems*, 282-286.

Lee, Y., Kim, S., Lee, Y. & Yoon, S. (2009). The performance analysis of CSS-based communication systems in the jamming environment. *World Academy of Science, Engineering and Technology 50, 2009*, 333-337.

Lin, Y., Peng,Y. & Wang, X. (2004). Maximum likelihood parameter estimation of multiple chirp signals by a new markov chain monte carlo approach. *Radar Conference, 2004. Proceedings of the IEEE*, 559-562.

MathWorks, alpha stable distributions in MATLAB (n.d.). Retrieved August 17, 2015, from http://math.bu.edu/people/mveillet/html/alphastablepub.html.

Nanotron Technologies, chirp spread spectrum (CSS), (n.d.). Retrieved from http://nanotron.com/EN/CO_techn-css.php.

Saha, S. & Kay, S.M. (2001). A noniterative maximum likelihood parameter estimator of superimposed chirp signals. *2001 IEEE International Conference on Acoustics, Speech, and Signal Processing, Proceedings. (ICASSP '01), 5*, 3109-3112.

Sahmoudi, M. & Meraim, K.A. (2004). Multicomponent chirp interference estimation for communication systems in impulsive alpha-stable noise environment. *First International Symposium on Control Communications and Signal Processing, 2004*, 299-302.

Salih, T.A. (2010). Performance analysis of chaotic chirp spread spectrum system in multi-path environment. *Journal of Theoretical and Applied Information Technology, 18*(2), 12-17.

Samorodnitsky, G. & Taqqu, M.S. (1994). *Stable non-Gaussian random processes: stochastic models with infinite variance*. Florida: CRC Press LLC.

Simic, I.S., Zejak, A.J. & Zrnic, B.M. (2001). Self intersymbol interference reduction in chirp spread spectrum communication systems. *IEEE International Conference on, EUROCON'2001, Trends in Communications, 2*, 525-527.

Springer, A., Huemer, M., Reindl, L., Ruppel, C.W., Pohl, A., Seifert, F., Gugler, W. & Weigel, R. (1998). A robust ultra-broad-band wireless communication system using SAW chirped delay lines. *IEEE Transactions on Microwave Theory and Techniques, 46*(12), 2213-2219.

Springer, A., Gugler, W., Huemer, M., Reindl, L., Ruppel, C.W. & Weigel, R. (2000). Spread spectrum communications using chirp signals. *IEEE/AFCEA EUROCOMM 2000. Information Systems for Enhanced Public Safety and Security*, 166-170.

Springer, A., Gugler, W., Huemer, M., Koller, R. & Weigel, R. (2001). A wireless spread-spectrum communication system using SAW chirped delay lines. *IEEE Transactions on Microwave Theory and Techniques, 49*(4), 754-759.

Sureka, G. & Kiasaleh, K. (2013). Sub-optimum receiver architecture for awgn channel with symmetric alpha-stable interference. *IEEE Transactions on Communications, 61*(5), 1926-1935.

Tutorial 1890, an introduction to spread-spectrum communications, (n.d.). Retrieved February 18, 2003, from https://www.maximintegrated.com/en/app-notes/index.mvp/id/1890.

Wang, X., Fei, M. & Li, X. (2008). Performance of chirp spread spectrum in wireless communication systems. *11th IEEE Singapore International Conference on Communication Systems, ICCS 2008*, 466-469.

Yang,F. & Zhang,X. (2014). BER analysis for digital modulation schemes under symmetric alpha-stable noise. *Military Communications Conference (MILCOM), 2014 IEEE*, 350-355.

Yifeng, S., Yongning, Z. & Lei, W. (2010). A fast estimation of multi-path delay using chirp signal. *2010 International Conference on Communications and Mobile Computing (CMC), 2*, 510-514.

Yu, X., Shi, Y. & Ma, Y. (2009). A cross fourth order moment minimum norm method for chirp time delay estimation. *International Conference on Mechatronics and Automation, ICMA 2009*, 2292-2296.

Zhang, W. & Tao, R. (2010). A time-fractional fourier joint representation-based parameter estimation method for chirp/frequency hopping spread spectrum signal. *First International Conference on Pervasive Computing Signal Processing and Applications (PCSPA)*, 1260-1263.

Zhang, P. & Liu, H. (2006). An ultra-wide band system with chirp spread spectrum transmission technique. *2006 6th International Conference on ITS Telecommunications Proceedings*, 294-297.

Zhao, Q., Zhang, Q. & Zhang, N.T. (2010). Multiple chirp-rate modulation based on fractional fourier transform. *First International Conference on Pervasive Computing Signal Processing and Applications (PCSPA)*, 688-691.

APPENDICES

MATLAB code

```
clc; clear all;
alpha=0.7; beta=0; gam=1; delta=0; Cg=1.78;
GSNR=-24:2:0;
BER_bok_tot=zeros(1,length(GSNR));
BER_pod_tot=zeros(1,length(GSNR));
BER_bok_tot_cauchy=zeros(1,length(GSNR));
BER_pod_tot_cauchy=zeros(1,length(GSNR));
Nbit=5e3; % the streaming bits
bitstream=2*(randint(1,Nbit)-.5);
% Transmitter stage
Rbit=1e6; % data bit rate
M_ary=2; k=1; Tb=log2(M_ary^k)/Rbit; % one bit duration
Tc=Tb; % chirp duration equals bit duration
fsamp=5e8; Tsamp=1/fsamp; % sampling frequency for Tc
fcent=2e7; % center frequency
Bw=4e6; % bandwidth of chirp signal
f1=fcent+Bw/2; f2=fcent-Bw/2; % initial and final frequencies
mu=Bw/Tc; % chirp rate
% Generated chirp signals
t=-(Tc/2-Tsamp):Tsamp:(Tc/2-Tsamp); % time span
sref=cos(2*pi*fcent*t+mu*pi*(t.^2));
sref0=cos(2*pi*fcent*t-mu*pi*(t.^2));
shift=10*log10(.5*length(sref)); % approximate 24 dB
RE=10;
for re=1:RE
re
for gsnr=1:length(GSNR)

%A=sqrt(2*(10^(GSNR(gsnr)/10))); % Only SaS Noise
A=sqrt(4*(10^(GSNR(gsnr)/10)));  % Gauss + SaS Noise
for n=1:Nbit
% chirp BOK scheme
sbok=A*cos(2*pi*fcent*t+bitstream(n)*mu*pi*(t.^2)); % reference signal
% chirp antipodal or BPSK scheme
spod=A*cos(2*pi*fcent*t+mu*pi*(t.^2)-bitstream(n)*(pi/2)+pi/2);
%----------channel-------------------------------
nn=stblrnd(alpha,beta,gam,0,1,length(sref));
nn_g=stblrnd(2,beta,gam,0,1,length(sref));
rbok=sbok+nn+nn_g;
rpod=spod+nn+nn_g;
```

```
est_bit_bok(n)=sign((sum(rbok.*sref)-sum(rbok.*sref0)));
est_bit_pod(n)=sign(sum(rpod.*sref));
est_bit_bok_cauchy(n)=sign(sum(log10((1./(pi*(1+(rbok-
sref).^2)))./(1./(pi*(1+(rbok-sref0).^2))))));
est_bit_pod_cauchy(n)=sign(sum(log10((1./(pi*(1+(rpod-
sref).^2)))./(1./(pi*(1+(rpod+sref).^2))))));
end
BER_bok(gsnr)=length(find(bitstream.*est_bit_bok<0))/Nbit;
BER_pod(gsnr)=length(find(bitstream.*est_bit_pod<0))/Nbit;
BER_bok_cauchy(gsnr)=length(find(bitstream.*est_bit_bok_cauchy<0))/Nbit;
BER_pod_cauchy(gsnr)=length(find(bitstream.*est_bit_pod_cauchy<0))/Nbit;
end
BER_bok_tot=BER_bok_tot+BER_bok;
BER_pod_tot=BER_pod_tot+BER_pod;
BER_bok_tot_cauchy=BER_bok_tot_cauchy+BER_bok_cauchy;
BER_pod_tot_cauchy=BER_pod_tot_cauchy+BER_pod_cauchy;
end
```